A synthesis of heat flow determinations and thermal modeling along the Nankai Trough, Japan

Robert Harris,[1] Makoto Yamano,[2] Masataka Kinoshita,[3] Glenn Spinelli,[4] Hideki Hamamoto,[5] and Juichiro Ashi[6]

Received 4 February 2013; revised 19 May 2013; accepted 23 May 2013; published 21 June 2013.

[1] We review marine heat flow data along the Nankai Trough and show that observations >30 km seaward of the deformation front are 20% below conductive predictions (129–94 mW m^{-2}) but consistent with the global heat flow average for oceanic crust of the same age (16–28 Ma). Heat flow values ≤30 km seaward of the deformation front are generally 20% higher than conductive predictions. This heat flow pattern is consistent with the advection of heat by fluid flow in the subducting oceanic crust and explains both the high heat flux in the vicinity of the trench, >200 and >140 mW m^{-2}, and steep landward declines to values of approximately 60 mW m^{-2} over distances of 65 and 50 km along the Muroto and Kumano transects, respectively. Along the Ashizuri transect, the lack of heat flow data precludes a definitive interpretation. We conclude that fluid flow in the subducting oceanic crust leads to temperatures that are generally 25°C higher near the toe of the margin wedge and 50–100°C lower near the downdip limit of the seismogenic zone than estimated by purely conductive models.

Citation: Harris, R., M. Yamano, M. Kinoshita, G. Spinelli, H. Hamamoto, and J. Ashi (2013), A synthesis of heat flow determinations and thermal modeling along the Nankai Trough, Japan, *J. Geophys. Res. Solid Earth*, *118*, 2687–2702, doi:10.1002/jgrb.50230.

1. Introduction

[2] The Nankai Trough of southwestern Japan (Figure 1) has been the site of numerous great earthquakes ($M_w > 8$) and is one of the best instrumented and most studied subduction zones in the world. There has been a significant quantity of geophysical and geological data collected in the region between Cape Ashizuri and the Kii Peninsula, including active reflection and refraction surveys, passive seismic studies, on-land GPS networks, and thermal data. Additionally, this region has been the site of many drilling projects through the Deep Sea Drilling Project (DSDP), the Ocean Drilling Program (ODP), and the Integrated Ocean Drilling Program (IODP). Currently, the focus of drilling is offshore of the Kii Peninsula along the Kumano transect (Figure 1) where the Nankai Trough Seismogenic Zone Experiment (NanTroSEIZE) is aimed at instrumenting the seismogenic portion of the subduction thrust, examining the thermal and hydrologic behavior of the plate boundary, and understanding the updip aseismic to seismic transition and the generation of earthquakes and tsunamis [*Tobin and Kinoshita*, 2006]. Prior to the NanTroSEIZE project, drilling concentrated offshore of Cape Ashizuri and Cape Muroto [*Karig et al*., 1975; *Kagami et al*., 1986; *Taira et al*., 1991; *Moore et al*., 2001; *Mikada et al*., 2002].

[3] One reason for investigating earthquakes along the Nankai margin is its long historical record of great thrust earthquakes that stretches back to 684 A.D. [*Ando*, 1975]. The recurrence interval for great earthquakes at this margin is 100 to 200 years with the most recent being the 1944 Tonankai ($M_w = 8.1$) and the 1946 Nankai ($M_w = 8.3$) subduction thrust events [*Kanamori*, 1972]. At accretionary margins, the transition from aseismic sliding to seismic stick-slip behavior is linked to mechanical changes in the underthrust sediment. As the initially weak sediments are lithified and thermally altered, they are better able to store elastic strain that can be released during a sudden slip event. Temperature along the subduction thrust is central to understanding the role of mechanical changes because of its influence on diagenesis, metamorphism, and fluid production [e.g., *Hyndman et al*., 1995; *Moore and Saffer*, 2001]. Other reasons for wanting to know the thermal regime of convergent margins include its influence on the occurrence of gas hydrates and, at depth, dehydration reactions in the subducted oceanic crust that lead to the generation of magma. At greater depths, the thermal regime influences petrology, magmatic processes, and intraslab earthquakes [*Peacock and Wang*, 1999; *Wada and Wang*, 2009].

[1]College of Earth, Oceanic, and Atmospheric Sciences, Oregon State University, Corvallis Oregon, USA.
[2]Ocean Hemisphere Research Center, University of Tokyo, Tokyo, Japan.
[3]Japan Agency for Marine-Earth Science and Technology, Yokosuka, Japan.
[4]Department of Earth and Environmental Science, New Mexico Institute of Mining and Technology, Socorro, New Mexico, USA.
[5]Center for Environmental Science in Saitama, Kazo, Japan.
[6]Atmosphere and Ocean Research Institute, University of Tokyo, Tokyo, Japan.

Corresponding author: R. Harris, College of Earth, Oceanic and Atmospheric Sciences, Oregon State University, 104 CEOAS Administration Bldg., Corvallis, OR 97331-5503, USA. (rharris@coas.oregonstate.edu)

2169-9313/13/10.1002/jgrb.50230

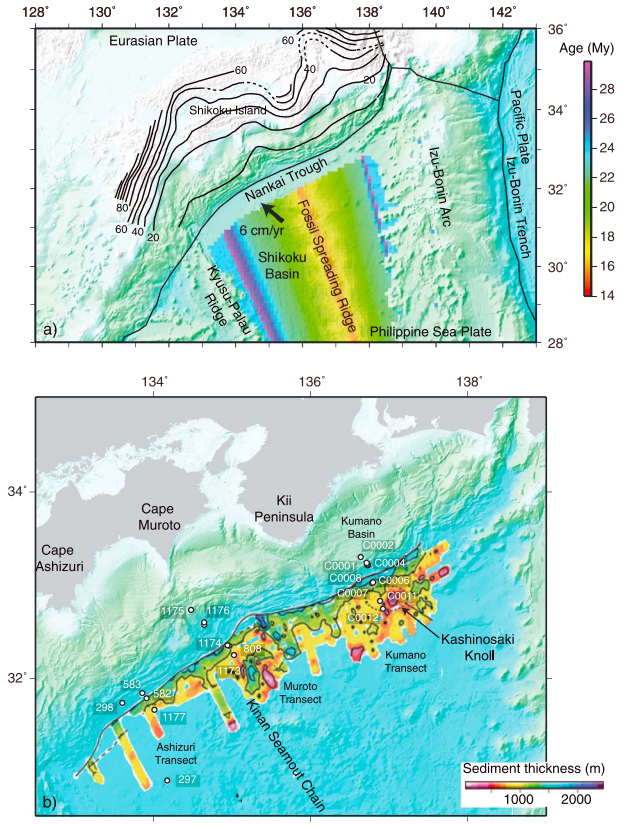

Figure 1. Tectonic setting of the Nankai Trough. (a) Location map showing the general bathymetry and crustal ages of Shikoku Basin [*Müller et al*., 2008]. Contours show estimated depth to top of the subducting Philippine Sea Plate [*Hirose et al*., 2008]. The contour interval is 10 km. (b) Detailed bathymetry and location of DSDP, ODP, and IODP boreholes. Sediment thickness from *Ike et al*. [2008] is shown.

[4] Sensitivity studies of subduction thermal models have found that the thermal regime of the shallow subduction zone is largely governed by the convergence rate, the slab geometry, and the thermal state of the incoming plate [e.g., *van den Beukel and Wortel*, 1988; *Dumitru*, 1991; *Molnar and England*, 1995; *Hyndman and Wang*, 1995; *McCaffrey*, 1997]. Thermophysical rock properties such as thermal conductivity and heat production are also important [*Dumitru*, 1991; *McCaffrey*, 1993]. In general, the convergence rate is well known from plate motion studies and the gross margin geometry and slab dip are estimated from active and passive seismic studies. The thermal structure of the incoming plate, particularly in the presence of hydrothermal circulation, and thermophysical rock properties at depth are generally less well known.

[5] The purpose of this paper is to assess the current state of knowledge of the thermal structure of the Nankai subduction zone by summarizing critical observations and reviewing thermal models of the margin. In doing this, we generate a regionally comprehensive and consistent interpretation of the thermal state of the Nankai subduction zone. We strive to develop a conceptual framework for the thermal state of the margin that is as simple as possible, yet consistent with observations. We hope this study stimulates additional research that helps address remaining ambiguities and questions.

2. Tectonic Setting

[6] The Nankai Trough, offshore of southwestern Japan, extends about 700 km from its intersection with the Izu-Bonin arc offshore of central Honshu to the Kyushu-Palau Ridge, a remnant arc (Figure 1). At the Nankai Trough, the Shikoku Basin (Philippine Sea Plate) is subducted beneath the Eurasian Plate.

[7] The geometry of the subducting plate influences the thermal regime of the subduction zone by controlling how steeply cold material descends. At shallow depths, the décollement has been mapped using wide-angle reflection and refraction surveys that span the Nankai Trough [*Kodaira et al*., 2000; 2002; *Baba et al*., 2002; *Nakanishi et al*., 2002]. These data resolve the plate boundary to depths of 15 to 20 km. Deeper, the structure has been estimated using receiver functions [*Shiomi et al*., 2004] and tomography [*Nakajima and Hasegawa*, 2007; *Hirose et al*., 2008]. These results have led to a number of models for the depth to the subducting slab [e.g., *Baba et al*., 2002; *Nakanishi et al*., 2002; *Wang et al*., 2004; *Hirose et al*., 2008], and although the details vary, they show similar undulations in the structure of the subducting slab (Figure 1). The Philippine Sea Plate shows a conspicuous trough under the Kii Peninsula and dips at a much shallower angle beneath Cape Ashizuri and Cape Muroto.

2.1. Characteristics of the Incoming Plate

2.1.1. Tectonic and Structural History

[8] The thermal regime of the incoming Philippine Sea Plate is intimately tied to the evolution of the Shikoku Basin crust and has been interpreted from drilling, gravity, magnetic, bathymetric, and regional plate kinematic data [*Watts and Weissel*, 1975; *Chamot-Rooke et al*., 1987; *Park et al*., 1990; *Taylor*, 1992; *Okino et al*., 1994, 1999; *Kobayashi et al*., 1995; *Sdrolias et al*., 2004].

[9] Prior to the opening of the Shikoku Basin, the old Pacific seafloor was subducting at the present position of the Shikoku Basin [*Sdrolias et al*., 2004]. With time, the trench-trench-trench triple junction formed by the Nankai Trough, the Izu-Bonin Trench, and the Japan Trench migrated to the northeast and passed in front of Shikoku Island at approximately 15 Ma. Since that time, Shikoku Basin crust has been subducting offshore of Shikoku Island. Subduction of the fossil ridge along the Nankai Trough is roughly parallel to the ridge's trend, so the age of the Philippine Sea Plate at the Nankai Trough increases with margin-parallel distance from the fossil ridge.

[10] *Sdrolias et al*. [2004] present a detailed analysis of the opening and motion of the Shikoku Basin. The Shikoku Basin formed through back-arc spreading associated with the Izu-Bonin subduction zone along a ridge system that propagated to the south [*Okino et al*., 1994]. Although the oldest recognizable crust in the Shikoku Basin is ~25 Ma, *Sdrolias et al*. [2004] infer that seafloor spreading initiated ~29 Ma based on a similar age of opening found in the Parece Vela Basin that forms the southern end of the Shikoku Basin. Assuming subduction rates of 20–40 km/Myr, they estimate that 300–600 km of the northern Shikoku Basin containing the oldest seafloor was subducted. DSDP and ODP drilling into the basin yield a Miocene age for the oldest sediments consistent with this interpretation. Spreading was ENE-WSW, appears to be symmetric,

and ceased ~15 Ma. Late-stage rifting may have continued until 7–10 Ma with associated volcanism that formed the Kinan Seamount Chain [*Chamot-Rooke et al*., 1987; *Ishii et al*., 2000]; alternatively post spreading eruption may have emplaced the Kinan seamounts along the fossil spreading axis [*Okino et al*., 1994]. The age of the youngest basalt dredged is estimated to be 10.1 ± 0.5 Ma and 7.6 ± 0.5 Ma from the Kii and Dai-ichi Kinan seamounts, respectively [*Ishii et al*., 2000].

[11] Changes in volcanic activity in western Japan have been used to suggest that subduction was very slow (<1 cm yr^{-1}) between 12 and 4 Ma and then increased to 4 cm yr^{-1} since about 4 Ma [*Kimura et al*., 2005]. Present-day subduction is approximately normal to the trough at a rate of about 4–6 cm yr^{-1} with more recent models indicating convergence rates near the high end of this range [e.g., *Seno et al*., 1993; *Miyazaki and Heki*, 2001; *Sella et al*., 2002; *DeMets et al*., 2010]. In this region, there are relatively few indicators of geologic plate motion rates and these rates are largely based on GPS monument velocities.

2.1.2. Sedimentation and Basement Relief

[12] The presence of sediments and their thickness can profoundly affect the thermal regime of the incoming plate in several ways [e.g., *Spinelli et al*., 2004]. In areas of fluid flow, low-permeability sediments control circulation patterns by blanketing areas of exposed basement, thereby restricting advection of basement fluids that can exchange heat with the overlying ocean. In general, because hydrologic driving forces are small (tens to hundreds kPa) and sediment permeability is low ($<10^{-17}$ m^2), sediment thickness of greater than a few meters is enough to suppress fluid flow between the basement and overlying ocean [*Fisher and Harris*, 2010]. In addition, the rapid deposition of cold sediments can transiently depress heat flow until the sediments warm to equilibrium conditions [e.g., *Hutchinson*, 1985]. Similarly, the removal of sediments through erosive or mass wasting events can transiently increase the heat flow until the unroofed material cools to equilibrium conditions.

[13] Seismic reflection and drilling data reveal patterns of sediment distribution and the stratigraphy of the Shikoku Basin and Nankai Trough [*Moore et al*., 2001; *Higuchi et al*., 2007; *Ike et al*., 2008]. In the Shikoku Basin, basement relief averages approximately 600 m and sediment thickness increases toward the Nankai Trough [*Chamot-Rooke et al*., 1987; *Higuchi et al*., 2007]. Sediment cover is discontinuous but can locally be as thick as 250 m in basement depressions [*Higuchi et al*., 2007]. Exposed basement is associated with topographic highs such as the Kinan Seamount Chain (Figure 1b).

[14] Within the Nankai Trough, terrigenous sediment is channeled along the trench axis from the Izu-Honshu collision zone toward the southwest. Along-strike variations in basement relief that include aseismic ridges, seamounts, and fracture zones lead to large variations in sediment thickness and deposition rates [*Ike et al*., 2008]. Southeast of the Kii Peninsula, basement relief is generally less than 600 m and maximum sediment thicknesses of approximately 1200 m is found in basement lows. Between the Kii Peninsula and Cape Muroto, including the Kinan Seamount Chain, basement is characterized by NW trending lows and large relief that can exceed 2 km. Sediment thickness can exceed 1 km. Between Cape Muroto and Cape Ashizuri, basement topography is more subdued with relief that varies between 200 and 400 m and sediment thicknesses generally less than 1 km.

3. Thermal Data

[15] Heat flow, q, is the product of the thermal conductivity (k) and the thermal gradient and in one dimension can be expressed as

$$q = -k\frac{\Delta T}{\Delta z}, \tag{1}$$

where $\Delta T/\Delta z$ is the vertical temperature gradient in sediments below the seafloor. Thermal conductivity measurements are made in situ with gravity-driven probes and in the laboratory with needle or divided bar apparatus. Thermal gradient measurements have been determined using gravity-driven probes, boreholes, and depths of bottom-simulating reflectors. We review each of these types of measurements below.

3.1. Thermal Conductivity

[16] Thermal conductivity exerts a fundamental influence on the distribution of temperatures (equation (1)) and is generally a function of mineralogy and porosity. Quartz-rich sand tends to have high thermal conductivities, whereas organic material, clays, and volcanic ashes have low thermal conductivity [e.g., *Zoth and Haenel*, 1988]. Thermal conductivity varies inversely with porosity because of the relatively low conductivity of water that fills the pores.

[17] Thermal conductivity is either measured in the shallow sub-bottom using gravity-driven probes [*Lister*, 1972] or on returned core material [*Von Herzen and Maxwell*, 1959; *Vacquier*, 1985; *Sass et al*., 1971, 1984] that allows measurements at greater depths than can be acquired with gravity-driven probes. For Nankai, where comparisons between core material and in situ values are available, agreement is good [*Yamano et al*., 2003; *Hamamoto et al*., 2011]. Laboratory techniques are summarized in *Harris et al*. [2011], and comparisons between these measurements for a series of boreholes comprising the Kumano transect found no systematic offsets. Experimental uncertainties for these measurements are estimated to be 3–5%.

[18] *Lin et al*. [2011] investigated the effects of pressure on thermal conductivity using core samples from the upper part of the accretionary prism at NanTroSEIZE Site C0001. Thermal conductivity increases with pressure at a rate of 0.014 W m^{-1} K^{-1} MPa^{-1}. This translates to an increase of about 7% and 20% for depths of 1 and 3 km, respectively.

[19] Seafloor values of thermal conductivity are relatively plentiful offshore of Cape Muroto and the Kii Peninsula but are less common offshore of Cape Ashizuri. Offshore of Cape Muroto, in situ and core values of thermal conductivity, extending a few meters below seafloor, are relatively uniform varying between 0.90 and 1.05 W m^{-1} K^{-1} with a mean value of 0.98 W m^{-1} K^{-1} [*Yamano et al*., 2003]. Offshore of the Kii Peninsula, marine probe and piston core measurements have a mean and standard deviation of 1.04 and 0.09 W m^{-1} K^{-1}, respectively ($n = 47$). For the entire data set, the mean and standard deviation of marine values are 1.0 ± 0.1 W m^{-1} K^{-1}. In general, no systematic trends in shallow values of thermal conductivity are observed and the mean and standard deviation of these values are 1.0 ± 0.1 W m^{-1} K^{-1}.

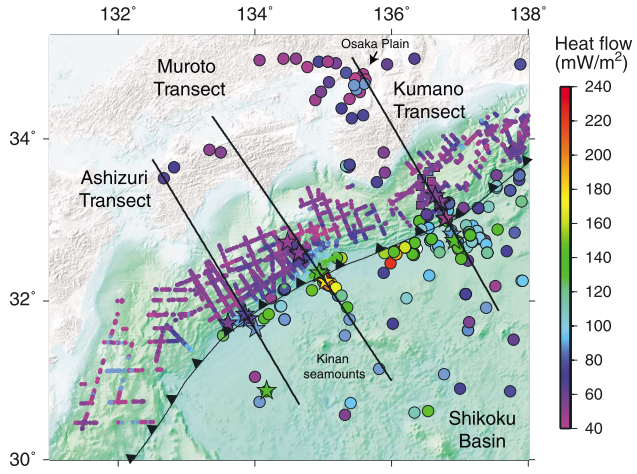

Figure 2. Heat flow measurements in the vicinity of the Nankai Trough. Marine probe (circles), boreholes (stars), and BSR (small circles) are color coded by heat flow. On land, circles show borehole values of heat flow. Black line at Muroto shows approximate location of *Wang et al.* [1995] and *Spinelli and Wang* [2008] models. Kumano transect line shows approximate position of thermal models [*Hyndman et al.*, 1995; *Hamamoto et al.*, 2011; *Harris et al.*, 2011; *Spinelli and Harris*, 2011; *Marcaillou et al.*, 2012].

[20] Values of thermal conductivity from greater depths accessible by drilling show variations due to both porosity and mineralogy. Thermal conductivity of incoming sediment at the reference drill sites, 1173, 1177, and C0011, varies between 1.0 W m^{-1} K^{-1} near the seafloor and 1.7 W m^{-1} K^{-1} at depths of several hundred meters to 1 km below the seafloor [*Moore et al.*, 2001; *Saito et al.*, 2010]. In general, thermal conductivity increases systematically with depth due to compaction. The greatest variability is associated with sandy turbidite intervals.

[21] Land values of thermal conductivity are made using a divided bar apparatus on rock chips or core samples or half-space probes on core faces. These values have a mean and standard deviation of 2.7 and 0.5 W m^{-1} K^{-1}, respectively. These values are higher than the marine values because of the low porosity and increased silica content.

3.2. Heat Flow From Gravity-Driven Probes

[22] Gravity-driven probe measurements of heat flow are relatively abundant in the Nankai Trough and these measurements have been summarized by *Watanabe et al.* [1970], *Yamano et al.* [1984], *Kinoshita and Yamano* [1986], and *Yamano et al.* [1992, 2003]. Heat flow probes used here are generally 4.5–6 m long with seven temperature sensors [*Yamano et al.*, 2003; *Kinoshita et al.*, 2008]. Because heat flow measurements at the seafloor are gradient measurements and because marine heat flow probes are relatively short, these measurements are susceptible to local environmental perturbations. Candidate sources of environmental perturbations to the background thermal field include sedimentation, erosion, bathymetric affects, bottom water temperature variations, and fluid advection. An additional source of uncertainty is that thermal conductivity was not measured at every site and instead heat flow values relied on nearby conductivity measurements. However, thermal conductivity values are relatively uniform across the area, so this practice likely introduces only small uncertainties.

[23] Variations in bottom water temperature diffuse into the sub-bottom distorting the geothermal gradient. To mitigate the effects of bottom water temperature variations, long-term measurements have been made offshore of Shikoku Island and the Kii Peninsula at water depths between 1000 and 2525 m. These temperature-time series show peak-to-peak amplitudes of 0.7°C and 0.3°C, respectively, over periods between 220 and 300 days [*Hamamoto et al.*, 2005, 2011]. At water depths of 2525 m, bottom water temperature variations can result in thermal gradient variations between the surface and 4 m of up to 25% [*Hamamoto et al.*, 2011] and may be larger at shallower depths.

[24] Heat flow measurements extend over the length of the Nankai Trough but are most dense offshore of Cape Muroto and the Kii Peninsula (Figure 2). Seaward of the Nankai Trough, heat flow measurements are more widely spaced than within the trough. Beginning with the earliest measurements of heat flow in the region, it was recognized that the Nankai Trough had higher heat flow than expected based on conductive cooling models parameterized in terms of seafloor age. Offshore of Cape Muroto, conductive cooling models predict heat flow should be approximately 130 mW m^{-2}; some measured values in this location exceed 200 mW m^{-2}. A second characteristic recognized with these surveys is that heat flow values show large local variability [*Watanabe et al.*, 1970].

3.3. Heat Flow From Marine Boreholes

[25] Seafloor drilling provides opportunities to measure the deeper temperature field (hundreds of meters to kilometers) that is less susceptible to shallow perturbations, but drilling costs preclude a spatially dense set of measurements. DSDP, ODP, and IODP have an extensive history of drilling along the Nankai Trough. Tools and techniques to measure formation temperatures in DSDP and ODP boreholes are summarized by *Pribnow et al.* [2000]. Formation temperatures are measured by inserting the temperature tool approximately 1 m ahead of the drill bit to minimize the drilling disturbance to the thermal field.

[26] The earliest ocean drilling heat flow measurements (Figures 1b and 2) are located offshore of Cape Ashizuri where heat flow was determined during DSDP Leg 31 at Sites 297 and 298 [*Karig et al.*, 1975]. Site 297 is in the north central part of the Shikoku Basin on the outer rise of the Nankai Trough and Site 298 is located on the lower inner slope of the Nankai Trough. Heat flow is 130–200 and 59 mW m^{-2} for Sites 297 and 298, respectively (Table 1). Both of these heat flow determinations are based on one temperature measurement below the seafloor and an estimated bottom water temperature. Additionally the thermal conductivity for Site 298 is estimated. Although these values are qualitatively consistent with high heat flow in the Nankai Trough and decreasing heat flow landward, they are quantitatively unreliable [*Yamano et al.*, 1992]. DSDP Leg 87 revisited the area offshore of Cape Ashizuri and drilled Sites 582 and 587 [*Kagami et al.*, 1986]. Site 582 is on the Nankai Trough floor slightly seaward of the deformation front and Site 583 is located at the prism toe (Figure 1b). Heat flow at Site 582 is based on four temperature measurements that extend to a depth of 508 m below seafloor (bsf) and yields a value of

Table 1. Borehole Values of Heat Flow[a]

Leg/Exp	Site	Latitude	Longitude	# Temp Meas	Max Depth (m bsf)	H.F. (mW m^{-2})	Sed Thick (m)	Gradient (°C/km)	Avg TC (W/m/K)	Bsmt Temp (°C)	Reference	Temperature Tools/Comments
						Ashizuri						
31	297	30.8767	134.1747	1	77	–	680	–	–	–	*Shipboard Sci. Party* [1975a]	DHI, not reliable
31	298	31.7258	133.6061	1	60	59	–	–	–	–	*Shipboard Sci. Party* [1975b]	DHI, not reliable
87	582	31.7752	133.9138	3	508	63	~750	46	1.35	35	*Shipboard Sci. Party* [1986a]; *Kinoshita and Yamano* [1986]	BWS
87	583	31.8333	133.8567	14	172	67	–	50	1.34	–	*Shipboard Sci. Party* [1986b]; *Kinoshita and Yamano* [1986]	BWS
190	1177	31.6525	134.0119		–	–	831	–	–	–	*Moore et al.* [2001]	DVTP, not reliable
						Muroto						
131	808	32.3500	134.9400	5	347	136	1290	111	–	112	*Taira et al.* [1991]	WSTP
190	1173	32.2444	135.0251	7	284	180	688	183	1.0	110	*Moore et al.* [2001]	APC
190	1174	32.3423	134.9565	2	65.5	183	–	183	1.0	–	*Moore et al.* [2001]	APC and DVTP
190	1175	32.5981	134.6446	4	383.5	56	–	54	1.0	–	*Moore et al.* [2001]	APC, DVTP, and WSTP
190	1176	32.5783	134.6446	5	273.9	54	–	56	1.0	–	*Moore et al.* [2001]	Adara APC and DVTP
190	1178	32.7310	134.4795	2	114.7	51	–	46	1.1	–	*Moore et al.* [2001]	WSTP
						Kumano						
315	C0001	33.2380	136.7117	7	171	60	–	44	–	–	*Harris et al.* [2011]	APCT3
315	C0002	33.3000	136.6367	6	159	57	–	40	–	–	*Harris et al.* [2011]	APCT3
316	C0004	33.2205	136.7222	5	135	54	–	52	–	–	*Harris et al.* [2011]	APCT3
316	C0006	33.0274	136.7938	6	277	45	–	27	–	–	*Harris et al.* [2011]	APCT3
316	C0007	33.0167	136.7830	5	81	70	–	42	–	–	*Harris et al.* [2011]	APCT3
316	C0008A	33.2137	136.7267	9	244	51	–	51	–	–	*Harris et al.* [2011]	APCT3
316	C0008C	33.2122	136.7279	10	139	53	–	57	–	–	*Harris et al.* [2011]	APCT3
333	C0011	32.8289	136.8818	9	184	89.5	1050	91.3	0.98	79	*Marcaillou et al.* [2012]	APCT3
333	C0012	32.7481	136.9171	10	174	141	538	139	1.01	64	*Marcaillou et al.* [2012]	APCT3
333	C0018	33.1570	136.6815	6	195	62	>320	70	0.89	–	*Marcaillou et al.* [2012]	APCT3

[a]# Temp Meas corresponds to the number of temperature measurements used to fit the thermal gradient, Max Depth corresponds to the depth of the maximum temperature measurement, H.F. is the heat flow, Sed Thick is the sediment thickness (only reported on incoming plate), Avg TC is the average thermal conductivity if given, Bsmt Temp is the estimated reported basement temperature (only reported on incoming plate), DHI is the downhole instrument, BWS is the Barnes water sampler, DVTP is the Davis-Villinger temperature probe, WSTP is the water sampler temperature probe, APC is the advanced piston corer tool, and APCT3 is the third generation advanced piston coring tool [*Pribnow et al.*, 2000].

63 mW m^{-2}. Assuming a sediment thickness of 750 m and a thermal gradient of 45.8° C km^{-1} gives a basement temperature of approximately 35° C. Heat flow at site 583 is based on 14 temperature measurements that reach depths of 172 m bsf and yields a value of 67 mW m^{-2}. Site 1177 was also drilled offshore of Cape Ashizuri during ODP Leg 190. Temperature values at Site 1177 are deemed unreliable [*Moore et al*., 2001]. Corrections for sedimentation and bathymetric relief have not been applied to these values such that these values may be 20% to 30% cooler than equilibrium [*Yamano et al*., 1992].

[27] Offshore of Cape Muroto, a total of six heat flow determinations were made during ODP Legs 131 and 190 [*Taira et al*., 1991; *Moore et al*., 2001]. Values of heat flow are based on two to seven equilibrium temperatures and many measurements of thermal conductivity. Heat flow was computed using thermal resistance that accounts for changes in the thermal gradient due to variations in thermal conductivity [*Bullard*, 1939]. In general, heat flow values based on drilling data are consistent with probe values, indicating that the high values of heat flow in the Nankai Trough are not due to shallow perturbations such as those introduced by changes in bottom water temperature. Heat flow in the trough floor varies between 183 and 136 mW m^{-2}; landward on the accretionary prism, heat flow decreases to values between 56 and 51 mW m^{-2} (Figure 2). These boreholes also provide information about the sedimentation history and suggest that these heat flow values may be about 20% cooler than equilibrium heat flow [*Yamano et al*., 1992]. An extrapolation of the observed thermal gradient at Site 808 suggests a basement temperature of approximately 112°C [*Taira et al*., 1991].

[28] Offshore of the Kii Peninsula, IODP Expeditions 315, 316, and 333 have resulted in a total of 11 borehole heat flow measurements [*Kinoshita et al*., 2011a; *Henry et al*., 2011]. Temperature was measured using either the third generation advanced piston coring tool (APCT3) [*Heesemann et al*., 2006] or the Davis-Villinger temperature probe (DVTP) [*Davis et al*., 1997a] and values of heat flow are based on between 4 and 10 equilibrium temperatures. Seaward of the deformation front, heat flow at C0011 and C0012 is 90 and 141 mW m^{-2}, respectively (Figure 1b). These values of heat flow when combined with thermal conductivity measurements yield sediment-basement temperature of 79°C and 65°C at Sites C0011 and C0012, respectively [*Henry et al*., 2011]. This variation in the temperature of the sediment-basement interface is attributed to fluid flow within the upper oceanic crust [*Henry et al*., 2011]. A detailed sedimentation correction indicates that the recent deposition of cold sediments may be depressing these values of heat flow by 11–13% [*Marcaillou et al*., 2012]. Landward of the trough, heat flow determinations, adjusted for the effects of sedimentation and bathymetric relief, generally decrease with landward distance and vary from 70 mW m^{-2} slightly landward of the deformation front to 57 mW m^{-2} at the Kumano Basin Site [*Harris et al*., 2011]. Corrections for sedimentation and bathymetric relief add between 5% and 28% to these values.

3.4. Heat Flow From Bottom Simulating Reflectors (BSRs)

[29] BSRs are commonly observed in seismic reflection profiles of continental margins [e.g., *Shipley et al*., 1979; *Kvenvolden*, 1993] and can be used to estimate heat flow. The position of BSRs is largely controlled by temperature and to a lesser extent by pressure. Estimates of heat flow are made by calculating the pressure at the BSR as the sum of the overburden load of seawater and the sediment column usually assuming hydrostatic pore pressures. Temperature at the BSR is based on a pressure-temperature phase diagram between methane and methane hydrate in the seawater. With knowledge of the seafloor temperature and estimates of the BSR depth through seismic reflection profiles, a thermal gradient can be determined and, coupled with an estimate of thermal conductivity, yields heat flow values [e.g., *Yamano et al*., 1982; *Hyndman et al*., 1992; *Ashi and Taira*, 1993; *Grevemeyer and Villinger*, 2001]. Measurements along the Nankai margin have been summarized by *Ashi and Taira* [1993] and *Ashi et al*. [2002].

[30] BSR estimates of heat flow are complementary to other techniques and offer several benefits. First, BSRs can significantly increase the spatial coverage of heat flow. Because both probe- and borehole-derived values of heat flow are relatively expensive, these measurements are relatively sparse. Second, because BSRs are generally a few hundred meters below the seafloor, they are less susceptible to seafloor perturbations such as short-term variations in bottom water temperature. Additionally, in areas where probe penetrations or boreholes are not possible because of submarine cables, BSRs allow estimates of heat flow to be made. However, because BSRs are indirect measures of heat flow, uncertainties tend to be relatively large. *Grevemeyer and Villinger* [2001] analyzed 10 ODP boreholes drilled through the gas hydrate stability field and formalized uncertainties in the estimation of heat flow. They find that if heat flow estimates from BSRs are calibrated with probe measurements, and a large data set of thermal conductivities is used, uncertainties in heat flow are less than 10%; otherwise, uncertainties can be 50–60%.

[31] BSRs have a long history of being used to estimate heat flow along the Nankai margin. *Yamano et al*. [1982] were the first to compute heat flow using observations of BSRs and showed that these values are consistent with probe values of heat flow. Later, ODP Site 808 penetrated the gas hydrate stability zone, and although no BSR was indicated at the site, one is present less than 3 km away [*Hyndman et al*., 1992]. *Hyndman et al*. [1992] used downhole temperatures, thermal conductivity, porosity, and logging data from Site 808 to test phase relationships for gas hydrate. They found good agreement (±5%) between observed and predicted temperatures at the base of the gas hydrate stability zone using a phase relationship for pure water and methane. Seafloor probe values of heat flow correspond to those estimated from the BSR to within 20% [*Yamano et al*., 1992]. These results suggest that heat flow estimates derived from BSRs at Nankai are reliable.

[32] BSRs are widely distributed within the prism slope and fore-arc basin at water depths between about 600 and 4650 m [*Ashi et al*., 2002]. Margin-wide patterns of heat flow estimated from BSRs reflect patterns similar to those observed with the probe and borehole determinations of heat flow (Figure 2). Values of heat flow decrease with distance landward of the trench and with distance from the fossil spreading ridge. The general landward decrease in heat flow reflects the thickening of the prism and the cooling effect of

the subducting plate, while the along-strike decrease reflects the aging of the oceanic crust from the fossil spreading center. *Ashi and Taira* [1993] found that BSR heat flow values were negatively correlated with the thickness of accretionary prism sediments and required the base of the sediment to be at a nearly uniform temperature of 120°C. However, where BSRs cross faults, they do not generally indicate the presence of advective fluid flow, as the BSRs do not bend away from the faults [*Ashi and Taira*, 1993].

[33] Although there is regionally good agreement between probe and borehole values of heat flow with BSR-derived values, local studies show that in some areas, BSRs appear to be out of thermal equilibrium with the regional temperature field [*Martin et al*., 2004; *Kinoshita et al*., 2011b]. These discrepancies are attributed to the combined effects of deformation, sedimentation, and/or erosion on the forearc slope.

3.5. Onshore Heat Flow

[34] Onshore heat flow data have been summarized by a number of authors [*Yamano and Kinoshita*, 1995; *Furukawa et al*., 1998; *Tanaka et al*., 2004]. On Shikoku Island, heat flow data are sparse; data are more abundant on the Kii Peninsula and to the west (Figure 2). With the exception of the Kii Peninsula where heat flow is relatively high [*Furukawa et al*., 1998], heat flow is low through the fore arc. On the Osaka Plain, low heat flow values (~40 mW m^{-2}) are attributed to a sedimentation or groundwater perturbation [*Nakagawa and Komatsu*, 1979]. Higher values (>120 mW m^{-2}) are associated with the volcanic arc or discharging warm water. Onshore heat flow values between Cape Ashizuri and the Kii Peninsula have a mean and standard deviation of 72 mW m^{-2} and 39 mW m^{-2}, respectively.

3.6. Heat Production

[35] Heat production is an important component of the total heat flow through continental crust, but it is generally undersampled. *Hyndman et al*. [1995] and *Wang et al*. [1995] derived values of heat production based on total gamma ray logging data from ODP Site 808C [*Taira et al*., 1991]. Using densities of 2700 kg m^{-3} and 2400 kg m^{-3}, they derived heat production values of 2.2 and 1.9 μW m^{-3} for continental rocks and marine sediments, respectively. Permian to Cretaceous accretionary sandstone and mudstone yield heat production values of 1.5 μW m^{-3} [*Yamaguchi et al*., 2001]. Heat production measurements of granitic samples from a borehole at the Nojimi fault in southwest Japan yield values of 1.6 μW m^{-3} [*Yamaguchi et al*., 2001] close to the average value for granitic rocks in southwest Japan of 1.8 μW m^{-3} [*Miyake et al*., 1975].

4. Heat Flow in the Shikoku Basin and Nankai Trough

[36] Globally, the first-order variation in heat flow in young (<65 Myr) oceanic crust can be understood in terms of lithospheric cooling with age superimposed with the advective effects of hydrothermal circulation [e.g., *Davis and Lister*, 1974; *Parsons and Sclater*, 1977; *Stein and Stein*, 1992, 1994; *Harris and Chapman*, 2004]. The vigor of circulation is primarily controlled by crustal permeability, basal heat flux, and distribution of exposed basement where fluids can recharge and discharge [*Davis and Elderfield*, 2004]. Vigorous hydrothermal circulation can cause extreme differences between nearby measurements, which can be explained in terms of variations in sediment thickness between nearly isothermal boundaries maintained by bottom water above and the sediment-basement interface below [*Davis et al*., 1989]. Ventilated hydrothermal circulation through upper basement is characterized by the flow of fluids between recharge and discharge areas leading to values that are on average lower than predicted. In areas of more complete sediment cover, insulated hydrothermal circulation may lead to values that are consistent with cooling reference models but still have a higher degree of scatter than can be explained with conductive heat transfer.

[37] We assess the thermal state of the incoming Shikoku Basin using the concept of fractional heat flow (q_{obs}/q_{pred}), where q_{obs} is the observed heat flow and q_{pred} is the predicted heat flow. We use a half-space cooling model to define q_{pred} [e.g., *Davis and Lister*, 1974] that can be expressed as

$$q_{pred} = \frac{C}{\sqrt{t}}, \tag{2}$$

where t is lithospheric age (Ma) and C is a constant that has been found to vary between about 473 and 510 mW m^{-2} ($Ma^{1/2}$) [*Parsons and Sclater*, 1977; *Stein and Stein*, 1992]. Following *Yamano and Kinoshita* [1995], we use a value of 500 mW m^{-2} ($Ma^{1/2}$) to compute q_{pred}. Back-arc basins may have a different thermal structure than normal oceanic lithosphere due to potential differences in spreading processes near the surface and mantle wedge processes at depth [*Currie and Hyndman*, 2006]. We assess whether the thermal state of the Shikoku Basin is consistent with the thermal structure of normal oceanic lithosphere, or anomalously warm as suggested for back-arc basins [e.g., *Currie and Hyndman*, 2006].

[38] Crustal ages associated with each heat flow measurement seaward of the deformation front have been assigned using the age grid of *Müller et al*. [2008]. In this region, the age grid is consistent with the tectonic reconstruction of *Sdrolias et al*. [2004] and has a resolution of 22 arc min and an uncertainty of about 5–6 Myr. The age grid (Figure 3a) does not extend through the trough to the deformation front and these values were assigned ages based on an extrapolation of the grid. Borehole biostratigraphic and paleomagnetic data from Sites 1173, 1177, and C0012 [*Moore et al*., 2001; *Saito et al*., 2010] indicate basement ages agree to within 3.5 Myr of ages extrapolated from the *Müller et al*. [2008] magnetic lineation-based grid.

[39] For observations more than 30 km seaward of the deformation front (Shikoku Basin values), the mean fractional heat flow is 0.8 (i.e., 20% below the predicted heat flow); these fractional values have a standard deviation of 0.4 (Figure 3a, inset). Figure 3b shows these values compared to global averages [*Stein and Stein*, 1994]. Average heat flow values in the Shikoku Basin are remarkably similar to global averages suggesting that this lithosphere has a thermal structure similar to the global average. The low mean and large standard deviation of heat flow values are consistent with ventilated hydrothermal circulation.

[40] Two other measures of the thermal state of oceanic lithosphere are variations in bathymetry and elastic thickness

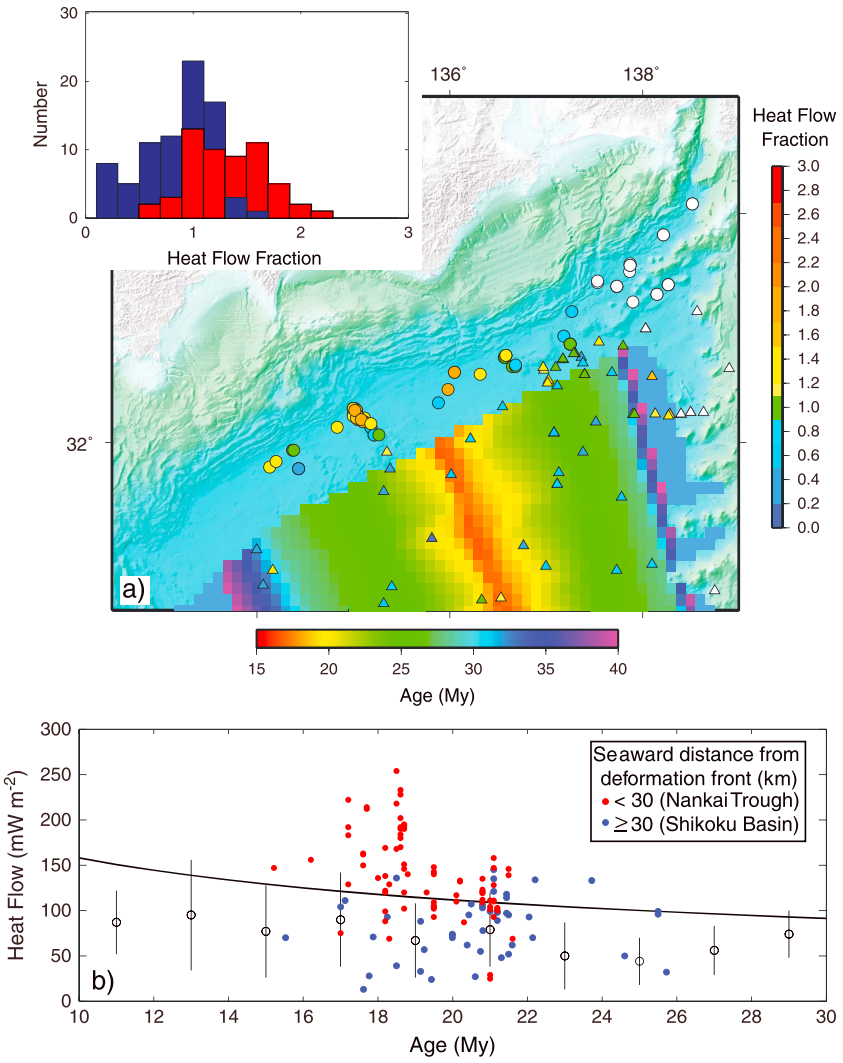

Figure 3. Heat flow data seaward of the deformation front. (a) Age grid of *Müller et al*. [2008] and fractional heat flow based on half-space cooling model. Data within 30 km of the deformation front are shown as circles and data greater than 30 km from the deformation front are shown as triangles. Inset shows histograms of heat flow fraction (the ratio of observed to half-space conductive prediction) for data greater than 30 km (blue) from the deformation front (mean = 0.84 ± 0.33) and data within 30 km (red) of the deformation front (mean = 1.20 ± 0.39). White circles indicate data beyond the edge of the age grid. (b) Heat flow as a function of age (small solid circles). Open circles show average global heat flow data grouped in 2 Myr bins [*Stein and Stein*, 1994]. Vertical bars show 1 standard deviation of the data. Line shows half-space cooling model.

as a function of crustal age. *Park et al*. [1990] evaluated bathymetric profiles in the Shikoku Basin and found that basement depths are approximately 800 m deeper than those of large ocean basins of the same age and that subsidence rates are similar. Values of elastic thickness determined at the Nankai Trough are also consistent with or thicker than the normal oceanic plate of this age [*Yoshioka and Ito*, 2001]. Both of these measures are inconsistent with an interpretation that the oceanic lithosphere is warmer than conductivity predictions.

[41] Due to the high rate of sedimentation within the Nankai Trough, heat flow values within 30 km of the deformation front (Nankai Trough values) are depressed relative to equilibrium values [*Yamano et al*., 2003]. *Marcaillou et al*. [2012] used magnetostratigraphic and nannofossil data from IODP Expeditions 322 and 333 [*Saito et al*., 2010; *Henry et al*., 2011] to estimate a sedimentation correction at IODP Sites C0011 and C0012. As sedimentation rates increase toward the trough, the correction increases from 11% at C0012, approximately 30 km from the deformation front, to 30% at the deformation front. These values are close to the 33% correction *Yamano et al*. [2003] calculated for Site 1173 and a regional 20% correction suggested by *Yamano and Kinoshita* [1995]. Even without these corrections, the fractional heat flow within the Nankai Trough (Figure 3a, inset) has a mean of 20% higher than the expected based on conductive cooling models and shows conspicuous scatter with a standard deviation of 0.4. The high mean fractional heat flow suggests an additional source of heat relative to conductive predictions that is landward of the Shikoku

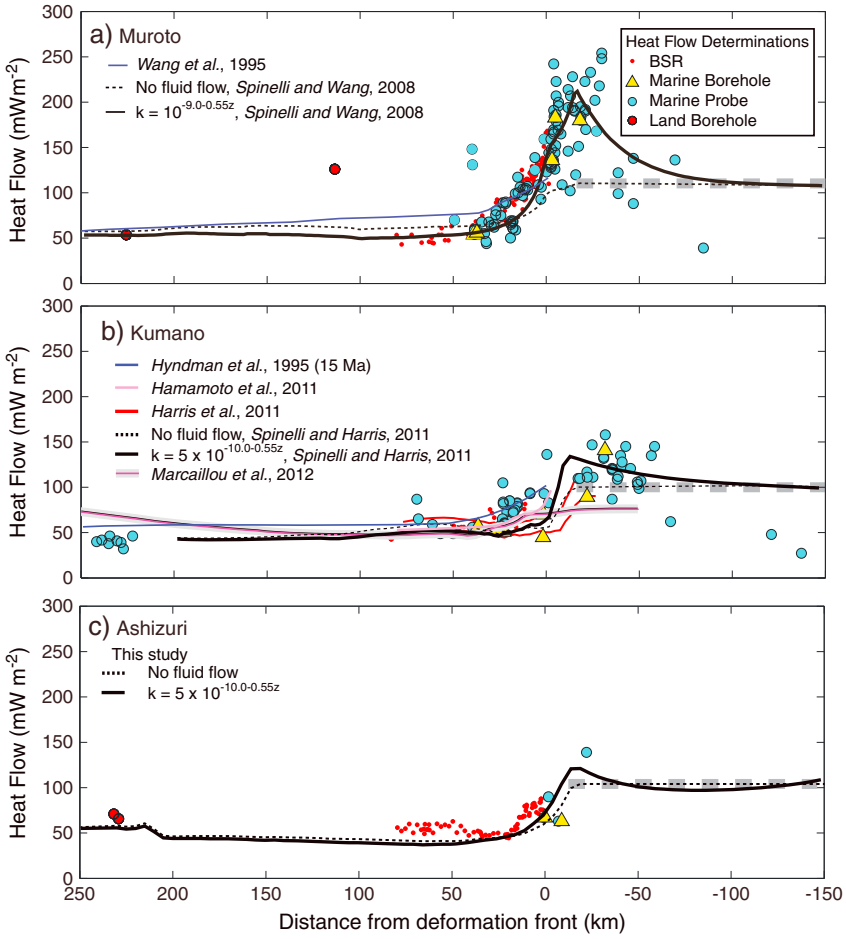

Figure 4. Heat flow data along the (a) Muroto, (b) Kumano, and (c) Ashizuri transects. The location is shown by black lines in Figure 3. Dashed gray lines show conductive prediction. Landward distances are positive. Lines show various thermal models for these transects.

Basin (i.e., either within the trench or the subduction zone). The large standard deviation in fractional heat flow in the trench is indicative of hydrothermal circulation.

[42] Figure 4 shows heat flow along the three drilling transects and illustrates three features discussed in previous compilations [*Yamano et al*., 1984, *Kinoshita and Yamano*, 1986; *Yamano et al*., 1992, 2003]: (1) relatively large variability between closely spaced heat flow measurements, (2) heat flow higher than conductive predictions within or just seaward of the Nankai Trough, and (3) a large and steep decrease in heat flow just landward of the deformation front. These features are best expressed in the Muroto transect where heat flow declines from values of approximately 210 mW m^{-2} near the deformation front to values of approximately 60 mW m^{-2} over a distance of 65 km. The steep landward descent in heat flow is less clear at Kumano. Here heat flow values decline from 140 mW m^{-2} to values of approximately 60 mW m^{-2} over a distance of 50 km. Although the sparseness of the data along the Ashizuri transect precludes a definitive statement about the presence of these features, the data are consistent with them.

5. Thermal Models of Subduction

[43] Many thermal models have been constructed along the Muroto and Kumano drilling transects using the finite element method as their basis. The popularity of finite element models is due its flexibility, both in the geometry of thermostratigraphic units, the plate interface, and in their thermal physical properties. Additionally, these models calculate temperatures for the entire system that can then be tested against deformation models constrained by geodetic data. In its most general form, this model solves the heat diffusion-advection equation to yield temperature, T, as a function of distance, x, depth, z, and time, t,

$$\nabla\cdot(k\nabla T) - \rho c\bar{v}\cdot\nabla T + Q = \rho c\frac{\partial T}{\partial t}, \qquad (3)$$

where k is thermal conductivity, ρc is volumetric heat capacity, and $\bar{v}$ is the convergence velocity. A heat source term Q is included that accounts for radiogenic heat production and frictional heating. As described later, many models use the steady state form of this equation (right-hand side set to 0) and small to negligible values of heat production. Most models are discretized into thermostratigraphic units (Figure 5) of varying complexity. Each element is assigned a constant thermal conductivity, heat generation, and heat capacity. The upper and lower boundaries are usually isothermal and set to 2°C and 1400°C, respectively. Small variations in these boundary values have negligible impact on the subduction thrust temperatures. For Nankai, the seaward boundary condition has been based on the half-space cooling

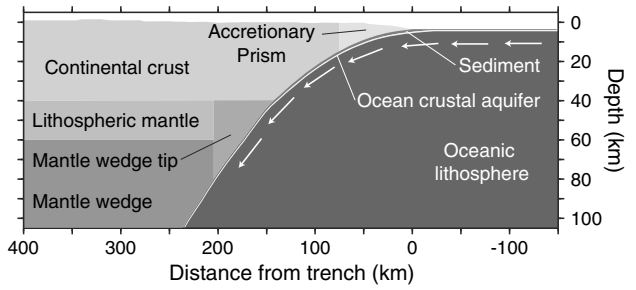

Figure 5. Schematic of model thermo unit used in finite element models. Not all models use all of these units.

model. The landward boundary condition is usually based on a steady state geotherm. In general, most models use similar thermophysical rock properties (Table 2). Sensitivity tests indicate that modest variations of parameters given in Table 2 have a small to negligible effect on temperatures along the subduction thrust [e.g., *Hyndman et al*., 1995; *Marcaillou et al*., 2012]. These models generally use the same incoming plate velocity of 40 to 50 mm yr^{-1}. All models use negligible values for the coefficient of friction with the exception of *Hamamoto et al*. [2011] that use a value of 0.05. For models that include the mantle wedge, isoviscous corner flow [*Batchelor*, 1967] is driven by the downgoing plate [e.g., *Currie et al*., 2004].

5.1. Muroto Transect

[44] Thermal models along the Muroto drilling transect sought to explain both the high heat flow in the trough and the rapid landward decrease in heat flow (Figure 4a). Explanations to account for the high heat flow values in the trough include (1) recent thermal rejuvenation by post spreading volcanism [*Yamano et al*., 1984]; (2) active fluid flow along the décollement and through underthrust sediments [*Yamano et al*., 1984; *Kinoshita and Yamano*, 1986; *Ashi and Taira*, 1993]; (3) sealing of the oceanic basement thereby changing hydrothermal circulation from ventilated seaward of the trench region to insulated within the trench region, and recovery of the geotherm [*Nagihara et al*., 1989]; and (4) hydrothermal circulation within the subducting oceanic crust [*Spinelli and Wang*, 2008]. The youngest volcanic rocks in the Kinan Seamount Chain are 7–10 Ma [*Sato et al*., 2002], but widespread thermal rejuvenation is inconsistent with the elastic flexure results [*Yoshioka and Ito*, 2001]. Fluid flow along the décollement and changing the style of hydrothermal circulation are insufficient to produce the large anomalous heat flow and the steep landward descent [*Yamano et al*., 1992, 2003].

[45] Early steady state models [*Honda and Uyeda*, 1983; *Kinoshita and Yamano*, 1995; *Furukawa*, 1995] were not able to adequately fit the data. *Wang et al*. [1995] used a time-dependent seaward boundary condition to explicitly simulate the transient thermal state caused by the subduction of the fossil spreading ridge. The transient model results in a better fit to the data, particularly landward of about 200 km, but failed to simulate the anomalously high trough values and the rapid landward decrease in heat flow.

[46] *Nagihara et al*. [1989] considered the impact of changing hydrothermal circulation patterns as continuity and thickness of the sediment cover increased with proximity to the trough. Within the Shikoku Basin, ventilated hydrothermal circulation is invoked to explain low values of heat flow. Near the trough, this pattern transitions to insulated circulation as hydrothermal heat exchange between the crust and ocean ceases. This modeling predicts a low heat flow in the Shikoku Basin and higher heat flow in the trench, but was not able to account for the anomalously high heat flow in the trench. *Nagihara et al*. [1989] concluded that an additional source of heat was needed to explain the very high heat flow values in the trench.

[47] *Spinelli and Wang* [2008] simulated the thermal effects of fluid circulation in the oceanic crust with a hydrothermal proxy, utilizing the Rayleigh number, *Ra*, and Nusselt number, *Nu*. *Ra* quantifies the tendency for convection in the aquifer; *Nu* measures the efficiency of advective heat transfer. Multiplying the intrinsic thermal conductivity of each aquifer element in a thermal model by *Nu* for the element approximates the efficient heat transport by hydrothermal circulation. This high thermal conductivity proxy is representative of heat

Table 2. Thermal Parameters Used in Modeling the Muroto, Kumano, and Ashizuri Transects

Thermal Unit	Thermal Conductivity (W/m/K)	Heat Production ($\mu W\ m^{-3}$)	Thermal Capacity ($MJ/m^3/K$)	Reference
Incoming sediments	1.5	1.5	2.5	*Harris et al*. [2011]; *Spinelli and Harris* [2011]; Ashizuri, this study
	1.0	1.5	2.5	*Marcaillou et al*. [2012]
Accretionary prism	1.5–2.5[a]	1.9–2.4[b]	2.5	*Wang et al*., [1995]; *Hyndman et al*., [1995]; *Harris et al*., [2011]; *Spinelli and Harris* [2011]; Ashizuri, this study
	1.9	1.5	2.5	*Marcaillou et al*. [2012]
	2.0	2.0	3.3	*Hamamoto et al*. [2011]
Continental crust upper, lower	2.5	1.9, 0.4	2.5	*Wang et al*., [1995]; *Hyndman et al*., [1995]
	2.5	0.4, 2.4[a]	2.5	*Harris et al*., [2011]; *Spinelli and Harris* [2011]; Ashizuri, this study
	2.2, 2.7	1.8, 0.2	2.5	*Marcaillou et al*. [2012]
Continental mantle upper, lower	2.5	0.0	2.5	*Wang et al*., [1995]; *Hyndman et al*., [1995]
	3.1	0.02	2.5	*Harris et al*., [2011]; *Spinelli and Harris* [2011]; Ashizuri, this study
	3.3	0.01	2.5	*Marcaillou et al*. [2012]
Oceanic crust/lithosphere	2.9	0.0	3.3	*Wang et al*., [1995]; *Hyndman et al*., [1995]
	3.1	0.02	3.3	*Harris et al*., [2011]; *Spinelli and Harris* [2011]; *Marcaillou et al*. [2012]; Ashizuri, this study
	3.0	0	3.3	*Hamamoto et al*. [2011]

[a]Thermal conductivity and heat production increases linearly from prism toe to backstop.
[b]Heat production decreases linearly from 0 to 10 km depth.

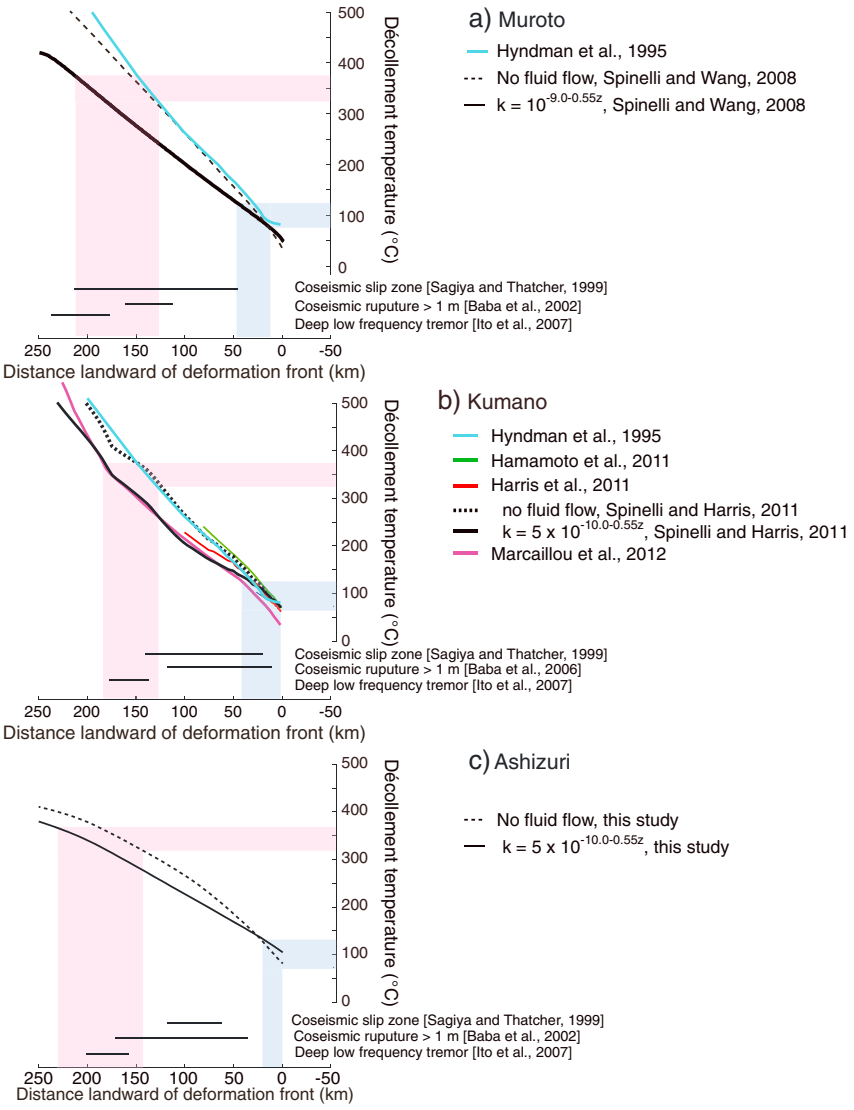

Figure 6. Modeled temperature along the subduction thrust at (a) Muroto and (b) Kumano. Shaded regions show the intersection of the $100 \pm 25°C$ (blue) and $350 \pm 25°C$ (red) isotherms with the subduction thrust and the horizontal spread implied by the models. The model of *Sagiya and Thatcher* [1999] likely includes the affect of after slip overestimating the size of the seismogenic zone.

transport via fluid circulation if $Nu > 20$ [*Davis et al*., 1997b], as it is for the oceanic crustal aquifer seaward of the trench and in the shallow subduction zone [*Spinelli and Wang*, 2008]. Their preferred model uses an aquifer in the upper oceanic crust that is 600 m thick and permeability function that decreases log linearly with depth from 10^{-9} m^2 at the trough to approximately 10^{-11} m^2 at 35 km. This model simulates the transport of heat from depth toward the trough within the upper oceanic crust. With this model, the heat exchange between the subducted and incoming crust explains both the high heat flow values in the trough and the rapid decrease in heat flow landward (Figure 4a) [*Spinelli and Wang*, 2008].

[48] Figure 6a shows temperature along the décollement for three models. The model of *Hyndman et al*. [1995] was constructed to the southwest of the *Spinelli and Wang* [2008] model where the plate interface dips less steeply and the décollement is cooler. The impact of fluid flow relative to no flow on the subduction interface is evident [*Spinelli and Wang*, 2008]. Relative to no flow conditions, fluid flow lowers temperatures on the subduction interface where heat is transported heat from depth and increases temperatures near the deformation front where heat is released.

5.2. Kumano Transect

[49] *Hyndman et al*. [1995] first modeled the thermal regime offshore of the Kii Peninsula by extending the modeling of *Wang et al*. [1995]. Their models showed how the thermal regime fit into the context of the downdip extent of the seismogenic zone but fail to capture some of the features of the newer thermal data including the low values of heat flow just landward of the deformation front (Figure 4b).

[50] *Hamamoto et al*. [2011] sought to quantify the shear stress on shallow plate interface. They parameterized their plate model using seismic reflection profiles [*Park et al*., 2002] and varied the magnitude of frictional heating and heat generation in the overriding plate. The seaward boundary condition used a geotherm based on half-space cooling for

a 20 Ma old plate. Their heat production in the overriding plate is 2.0 μW m^{-3}, a value consistent with the heat production of Shikoku Basin sediment determined from ODP Hole 808C [*Taira et al*., 1991; *Hyndman et al*., 1995]. The effective coefficient of friction is less than 0.1 suggesting a very low shear stress supporting the assumption of negligible frictional used in models of the Kumano transect.

[51] *Harris et al*. [2011] parameterized the model geometry using the *Moore et al*. [2009] seismic reflection profile and tomographic imaging for the deeper slab geometry [*Hirose et al*., 2008]. They focused on the influence of the incoming plate geotherm and developed a warm and cool scenario corresponding to half-space cooling geotherms for 10 and 20 Ma crust. The 10 Ma crust was justified on the basis of the fit to the data in the Nankai Trough and arguments that back-arc basins may be warmer than normal oceanic basins. This range in thermal models appears to capture the range in heat flow values collected at IODP Sites (Figure 4b). However, our more complete analysis of heat flow seaward of the Nankai Trough no longer supports the interpretation of higher heat flow being due to a younger thermal age.

[52] *Spinelli and Harris* [2011] investigated the effect of hydrothermal circulation in the subducting oceanic crust along the Kumano transect using the hydrothermal proxy developed by *Spinelli and Wang* [2008]. The permeability structure of the subducting oceanic crust has a large impact on the simulated heat flow and temperature structure along the décollement. They used a permeability function that decreases with depth from 5×10^{-10} m^2 at the trough to 10^{-12} m^2 at 35 km. These permeability values are lower than those used at Muroto consistent with the older seafloor at Kumano. This model (Figure 4b) captures the high heat flow just seaward of the Nankai Trough and the rapid landward descent in heat flow.

[53] *Marcaillou et al*. [2012] used drilling results from Sites C0011 and C0012 to develop detailed thermal models of the rapid sedimentation caused by turbidites. They show that the very high sedimentation rates near the deformation front lead to cooler temperatures along the subduction thrust than other thermal models with the same amount of sediment but with lower sedimentation rates (Figure 6b). *Marcaillou et al*. [2012] also invoked higher heat flow for the Shikoku Basin based on its back-arc origin.

[54] The suite of models shown in Figure 4b shows a range in predicted heat flow that generally fit the observed data. Temperatures along the subduction thrust for each of these models show modest variation that generally increases with distance from the deformation front (Figure 6b). At the deformation front, the spread in model temperatures is about 45°C, at 100 km it is about 60°C, and at 200 km the spread is about 85°C. At a distance greater than 100 km from the deformation front, there are little data to constrain these models. At C0002 where drilling is planned to intersect the seismogenic zone temperatures, estimated temperatures range between 75°C and 115°C. The source of these variations stems from the different interface geometries, the magnitude of the sedimentation correction, and fluid flow within the upper oceanic crust. For example, the *Hamamoto et al*. [2011] model has the warmest temperatures along the subduction thrust (Figure 6b) and is likely a consequence of having both the deepest subduction thrust geometry and frictional heating. In general, the coldest models are those of *Spinelli and Harris* [2011] and *Marcaillou et al*. [2012] that invoke crustal fluid flow or rapid sedimentation near the trench, respectively. Although both of these processes act to lower temperature on the subduction thrust, they have opposite effects on surface heat flow. Rapid sedimentation decreases heat flow until the newly deposited sediments can warm to equilibrium. In contrast, because fluid flow within the subducting oceanic crust brings heat from depth toward the surface, surface values of heat flow are increased. The difference in these models is evident in Figure 4b where the hydrothermal model values of heat flow are above the conductive prediction and the rapid sediment model values of heat flow are significantly below the conductive prediction. These figures show that these models are most sensitive to these differences near the deformation front.

5.3. Ashizuri Transect

[55] To test the idea that fluid flow within the subducting oceanic crust is also occurring along the Ashizuri transect, we present thermal models using parameters consistent with those along the Kumano transect. The model geometry is based on the seismic velocity model of *Takahashi et al*. [2002]. Seaward of Cape Ashizuri, the oceanic plate has a crustal thickness of 6 km and deepens from 6.1 km at the trench to approximately 20 km at the coastline, 140 km from the deformation front. The angle of the subducting plate is approximately constant with a dip of 7° [*Takahashi et al*., 2002]. The sediment thickness at the deformation front is 750 m. This structure is represented in a 2-D finite element mesh that extends from 150 km seaward of the trench to 400 km landward. The landward boundary is placed sufficiently far from the region of interest to avoid edge effects. Seaward of the trench, the mesh has a horizontal surface to aid in the evaluation of the thermal structure of the incoming plate. The model is divided into five thermostratigraphic units: marine sediments, accretionary wedge, upper continental crust, lower continental crust, mantle wedge, and oceanic plate (Table 2). We use a maximum crustal thickness of 30 km. Temperature at the upper boundary of the model is fixed at 0°C and at the base of the oceanic lithosphere is fixed at 1400°C. At the landward boundary, we use a geotherm consistent with a back-arc setting; the landward boundary is far from the region of interest to avoid boundary effects. At the seaward boundary (150 km from the trench), we use a geotherm for 20 Ma conductively cooled oceanic lithosphere. Flow in the mantle wedge between the two converging plates is kinematically introduced using the analytical corner flow solution described by *Peacock and Wang* [1999]. The wedge flow results in a warm back arc, but it has little effect on the fore-arc thermal regime.

[56] We show two thermal models (Figure 4c), the first with no fluid flow in the oceanic crust and the second using the hydrothermal proxy to simulate fluid flow in a 600 m thick aquifer at the top of the oceanic plate following the procedure developed by *Spinelli and Wang* [2008]. We use the same permeability function at Ashizuri as that used at Kumano [*Spinelli and Harris*, 2011]. Heat flow values along the Ashizuri transect are sparse and it appears that either model can be argued to be consistent with the data.

[57] Temperatures along the subduction thrust at Ashizuri show similar patterns to those observed at Muroto (Figure 6c). The fluid flow model shows that heat is removed from deep in the system decreasing temperatures at depth and this heat is

advected toward the trough where it warms temperatures along the subduction thrust.

5.4. Fluid Flow in Subduction Crust Along the Nankai Trough

[58] A key question posed by these models is whether the flow system modeled at Muroto extends along the Nankai Trough between the Ashizuri and Kumano transects. The Nankai Trough has long been considered anomalously warm with respect to conductive predictions [*Yamano et al*., 1984, 2003]. Although heat flow is expected to decrease landward over the accretionary prism due to thickening of the accretionary prism and the downward advection of the cold subducting plate, the steep landward descent in heat flow, most conspicuous along the Muroto transect, has been difficult to explain. That fluid flow is occurring in oceanic crust less than 65 Ma is not surprising. Advecting heat upward with convecting fluids within the subducting oceanic aquifer provides a single mechanism to both warm the trench and cool the shallow subduction zone, explaining both prominent heat flow anomalies on the margin [*Spinelli and Wang*, 2008].

[59] Thermal models not including fluid flow in the subducting oceanic crust have not successfully described the large heat flow anomaly or its sharp landward decline [*Spinelli and Wang*, 2008]. At Kumano, the data are somewhat less compelling than at Muroto, but fluid flow is consistent with the high heat flow values seaward of the Nankai Trough and the landward decline of heat flow (Figure 4b). The modeled fluid flow associated with the Kumano transect is less vigorous than at Muroto and this may be due to the older age of oceanic crust along the Kumano transect. The data along the Ashizuri transect are too sparse to make a definitive discrimination between the conductive and fluid flow thermal models. These fluid flow models at Kumano and Ashizuri can be tested with additional heat flow data in the Nankai Trough and seaward of it.

5.5. Relationship Between Temperature and the Seismogenic Zone

[60] The Nankai Trough at Muroto and Kumano is one of the first places where it was hypothesized that the seismogenic zone along the subduction thrust is bounded within a specific temperature range [*Hyndman et al*., 1995, 1997]. The updip extent appears to be bounded by the 100–150°C isotherm and the downdip extent appears bounded by the 350°C isotherm or the intersection of the subduction thrust with the fore-arc mantle and has now been observed at many convergent margins [e.g., *Oleskevich et al*., 1999; *Harris and Wang*, 2002; *Currie et al*., 2002; *Manea et al*., 2004; *Hippchen and Hyndman*, 2008; *Harris et al*., 2010].

[61] Figure 6 shows estimates of the seismogenic zone along the Muroto, Kumano, and Ashizuri transects. The width of the coseismic zone of the 1944 Tonankai ($Mw = 8.1$) and 1946 Nankaido ($Mw = 8.3$) earthquakes has been estimated using geodetic survey measurements [*Sagiya and Thatcher*, 1999; *Liu et al*., 2010] and tide gauge tsunami data [*Baba et al*., 2002, 2006]. Differences between these estimates for the seismogenic zone may be ascribed to the differences in temporal sensitivity of these measures, tide gauge data represent short-term estimates of deformation (few months), whereas geodetic leveling data represent the seismogenic zone over a 3–5 year period. The model of *Sagiya and Thatcher* [1999] likely includes the affect of after slip and the model of *Liu et al*., [2010] assumes an elastic Earth. The impact of not specifically including viscoelastic rheology in models of the subduction earthquake cycle may make these seismogenic zone estimates too large [*Wang et al*., 2012]. Nevertheless, estimates of the seismogenic zone are generally consistent with the hypothesized 100°C and 350°C isotherms in Muroto and Kumano (Figure 6) as noted in previous studies [e.g., *Hyndman and Wang*, 1995]. The observed slip zone at Ashizuri is smaller than the thermally defined seismogenic zone at Ashizuri, but this could be because the thermal models are poorly estimated or that the entire seismogenic zone has not been observed. This figure shows that models including hydrothermal circulation in the subducted crust tend to decrease temperatures over the width of the seismogenic zone.

[62] Correlations between temperature and the seismogenic zone indicate that precisely and accurately estimating subduction thrust temperatures is important to understanding processes along the fault zone. The relationship between the downdip limit and temperatures near 350°C is generally understood in terms of the brittle-ductile transition. However, this region exhibits more complex behavior than previously thought. Episodic slow slip, low-frequency earthquakes, and seismic tremor are now identified in the deep seismic to aseismic transition zone [*Obara*, 2002; *Obara et al*., 2004; *Hirose and Obara*, 2005; *Ito et al*., 2007]. Hypocenters of VLF earthquake have an average depth and standard deviation of 40 ± 8 and 35 ± 9 in the Kii-Tokai and Shikoku regions, respectively [*Ito et al*., 2007].

[63] Similarly, understanding the updip aseismic to seismic transition has also been challenging. Many candidate processes responsible for the transition from aseismic sliding to stick-slip behavior have been identified [e.g., *Moore and Saffer*, 2001] and the transition may well be influenced by processes only indirectly depending on temperature or not at all. Finally, these deformation events and thermal models of subduction zones are relatively coarse (on the order of kilometers or more). Given the relatively broad spread of estimated temperatures along the subduction thrust as suggested by these models, progress in understanding the role of mechanical changes to fault zone rocks will likely require drilling and in situ fault zone monitoring as envisioned in NanTroSEIZE.

6. Conclusions

[64] On the basis of this review, we conclude the following:

[65] 1. Marine heat flow values greater than 30 km seaward of the Nankai deformation front have a fractional heat flow (q_{obs}/q_{pred}) with a mean and standard deviation of 0.8 and 0.4, respectively. Mean values are consistent with global averages for the same age. These observations indicate the presence of vigorous hydrothermal circulation and suggest that the thermal structure of the Shikoku Basin crust is similar to global averages for the same crustal age.

[66] 2. Within 30 km of the deformation front, the mean and standard deviation of fractional heat flow are 1.2 and 0.4, respectively. The high fractional heat flow suggests an added source of heat relative to conductive predictions and the large standard deviation suggests advective fluid flow.

[67] 3. The high heat flow values within the Nankai Trough and the anomalously steep drop in heat flow on the margin

wedge are consistent with fluid flow in the upper oceanic crust of the subducting plate. This observation has been made previously at Muroto [*Spinelli and Wang*, 2008] but is also suggested by this analysis at Kumano and is consistent with data at Ashizuri. Thus, fluids from depth may be heating sediments within the Nankai Trough along its length at least between the Ashizuri and Kumano transects. The implication of this conclusion is that temperatures along the subduction thrust are higher near the toe and lower landward of the deformation front than estimated by models not including hydrothermal circulation.

[68] **Acknowledgments.** We thank K. Wang, an anonymous reviewer, and the Associate Editor for comments and insights that improved this study. This research was supported by the Consortium for Ocean Leadership and National Science Foundation grant NSFOCE0637120 to G.A.S. and through the U.S. Science Support Program for IODP (NSF 0652315) that is administered by the Consortium for Ocean Leadership to R.N.H.

References

Ando, M. (1975), Source mechanisms and tectonic significance of historical earthquakes along the Nankai Trough, Japan, *Tectonophysics*, *27*, 119–140, doi:10.1016/0040-1951(75)90102-X.

Ashi, J., and A. Taira (1993), Thermal structure of the Nankai accretionary prism as inferred from the distribution of gas hydrate BSRs, in *Thermal Evolution of the Tertiary Shimanto Belt, Southwest Japan: An Example of Ridge-Trench Interaction*, Spec. Pap. Geol. Soc. Am., *273*, 137–149.

Ashi, A., H. Tokuyama, and A. Taira (2002), Distribution of methane hydrate BSRs and its implication for the prism growth in the Nankai Trough, *Mar. Geol.*, *187*, 177–191, doi:10.1016/S0025-3227(02)00265-7.

Baba, T., Y. Tanioka, P. R. Cummins, and K. Uhira (2002), The slip distribution of the 1946 Nankai earthquake estimated from tsunami inversion using a new plate model, *Phys. Earth Planet. Inter.*, *132*, 59–73, doi:10.1016/S0031-9201(02)00044-4.

Baba, T., P. R. Cummins, T. Hori, and Y. Kaneda (2006), High precision slip distribution of the 1944 Tonankai earthquake inferred from tsunami waveforms: Possible slip on a splay fault, *Tectonophysics*, *426*, 119–134.

Batchelor, G. K. (1967), *An Introduction to Fluid Dynamics*, 635 pp., Cambridge Univ. Press, New York.

Bullard, E. C. (1939), Heat flow in South Africa, *Proc. R. Soc. London, Ser. A*, *173*, 474–502, doi:10.1098/rspa.1939.0159.

Chamot-Rooke, N., V. Renard, and X. Le Pichon (1987), Magnetic anomalies in the Shikoku Basin: A new interpretation, *Earth Planet. Sci. Lett.*, *93*, 214–228, doi:10.1016/0012-821X(87)90067-7.

Currie, C. A., and R. D. Hyndman (2006), The thermal structure of subduction zone back arcs, *J. Geophys. Res.*, *111*, B08404, doi:10.1029/2007JB005415.

Currie, C., R. Hyndman, K. Wang, and V. Kostoglodov (2002), Thermal models of the Mexico subduction zone: Implications for the megathrust seismogenic zone, *J. Geophys. Res.*, *107*(B12), 2370, doi:10.1029/2001JB000886.

Currie, C., K. Wang, R. D. Hyndman, and J. He (2004), The thermal effects of steady-state slab-driven mantle flow above a subducting plate: The Cascadia subduction zone and back arc, *Earth Planet. Sci. Lett.*, *223*(1–2), 35–48.

Davis, E. E., and H. Elderfield (2004), *Hydrogeology of the Oceanic Lithosphere*, 706 pp., Cambridge Univ. Press, New York.

Davis, E. E., and C. R. B. Lister (1974), Fundamentals of ridge crest topography, *Earth Planet. Sci. Lett.*, *21*, 405–413.

Davis, E. E., D. S. Chapman, C. B. Forster, and H. Villinger (1989), Heat-flow variations correlated with buried basement topography on the Juan de Fuca ridge flank, *Nature*, *342*, 533–537.

Davis, E. E., H. Villinger, R. D. MacDonald, R. D. Meldrum, and J. Grigel (1997a), A robust rapid-response probe for measuring bottom-hole temperatures in deep-ocean boreholes, *Mar. Geophys. Res.*, *19*, 267–281.

Davis, E. E., K. Wang, J. He, D. S. Chapman, H. Villinger, and A. Rosenberger (1997b), An unequivocal case for high Nusselt number hydrothermal convection in sediment-buried igneous oceanic crust, *Earth Planet. Sci. Lett.*, *146*(1), 137–150.

DeMets, C., R. G. Gordon, and D. F. Argus (2010), Geologically current plate motions, *Geophys. J. Int.*, *181*(1), 1–80.

Dumitru, T. A. (1991), Effects of subduction parameters on geothermal gradients in fore arcs with an application to Franciscan subduction in California, *J. Geophys. Res.*, *96*, 621–641, doi:10.1029/90JB01913.

Fisher, A., and R. Harris (2010), Using seafloor heat flow as a tracer to map subseafloor fluid flow in the ocean crust, *Geofluids*, *10*(12), 142–160.

Furukawa, Y. (1995), Temperature structure in the crust of the Japan arc and the thermal effects of subduction, in *Terrestrial Heat Flow and Geothermal Energy in Asia*, edited by M. L. Gupta and M. Yamano, pp. 203–219, Oxford and IBH, New Delhi.

Furukawa, Y., H. Shinjoe, and S. Nishimura (1998), Heat flow in the southwest Japan arc and its implications for thermal processes under arcs, *Geophys. Res. Lett.*, *25*, 1087–1090.

Grevemeyer, I., and H. Villinger (2001), Gas hydrate stability and the assessment of heat flow through continental margins, *Geophys. J. Int.*, *145*, 647–660, doi:10.1046/j.0956-540x.2001.01404.x.

Hamamoto, H., M. Yamano, and S. Goto (2005), Heat flow measurement in shallow seas through long-term temperature monitoring, *Geophys. Res. Lett. 32*, L21311, doi:10.1029/2005gl024138.

Hamamoto, H., M. Yamano, S. Goto, M. Kinoshita, K. Fujino, and K. Wang (2011), Heat flow distribution and thermal structure of the Nankai subduction zone off the Kii Peninsula, *Geochem. Geophys. Geosyst.*, *12*, Q0AD20, doi:10.1029/2011GC003623.

Harris, R. N., and D. S. Chapman (2004), Deep-seated oceanic heat flux, heat deficits and hydrothermal circulation, in *Hydrology of the Oceanic Lithosphere*, edited by E. Davis and H. Elderfield, pp. 311–336, Cambridge Univ. Press, Cambridge, U. K.

Harris, R. N., and K. Wang (2002), Thermal models of the Middle America trench at the Nicoya Peninsula, Costa Rica, *Geophys. Res. Lett.*, *29*(21), 2010, doi:10.1029/2002GL015406.

Harris, R. N., G. Spinelli, C. R. Ranero, I. Grevemeyer, H. Villinger, and U. Barckhausen (2010), Thermal regime of the Costa Rican convergent margin: 2. Thermal models of the shallow Middle America subduction zone offshore Costa Rica, *Geochem. Geophys. Geosyst.*, *11*, Q12S29, doi:10.1029/2010GC003273.

Harris, R. N., F. Schmidt-Schierhorn, and G. A. Spinelli (2011), Heat flow along the NanTroSEIZE transect: Results from IODP Expeditions 315 and 316 offshore the Kii Peninsula, Japan, *Geochem. Geophys. Geosyst.*, *12*, Q0AD16, doi:10.1029/2011gc003593.

Heesemann, M., H. Villinger, A. T. Fisher, A. M. Tréhu, and S. White (2006), Data report: Testing and deployment of the new APCT-3 tool to determine in situ temperatures while piston coring, in *Cascadia Margin Gas Hydrates*, edited by M. Riedel et al., Proc. Integr. Ocean Drill. Program, *311*, doi:10.2204/ iodp.proc.311.108.2006.

Henry, P., T. Kanamatsu, and the Expedition 333 Scientists (2011), NanTroSEIZE State 2: NanTroSEIZE, Leg 333, Expedition Reports, *Proc. Integr. Ocean Drill. Program*, *333*.

Higuchi, Y., Y. Yanagimoto, K. Hoshi, S. Unou, F. Akiba, K. Tonoike, and K. Koda (2007), Cenozoic stratigraphy and sedimentation history of the northern Philippine Sea based on multichannel seismic reflection data, *Island Arc*, *16*, 374–393, doi:10.1111/j.1440-1738.2007.00588.x.

Hippchen, S., and R. Hyndman (2008), Thermal and structural models of the Sumatra subduction zone: Implications for the megathrust seismogenic zone, *J. Geophys. Res.*, *113*, B12103, doi:10.1029/2008JB005698.

Hirose, H., and K. Obara (2005), Repeating short- and long-term slow slip events with deep tremor activity around the Bungo channel region, southwest Japan, *Earth Planets Space*, *57*, 961–972.

Hirose, F., J. Nakajima, and A. Hasegawa (2008), Three-dimensional seismic velocity structure and configuration of the Philippine Sea slab in southwestern Japan estimated by double-difference tomography, *J. Geophys. Res.*, *113*, B09315, doi:10.1029/2007JB005274.

Honda, S., and S. Uyeda (1983), Thermal processes in subduction zones—A review and preliminary approach on the origin of arc volcanism, in *Arc Volcanism: Physics and Tectonics*, edited by D. Shimozuru and I. Yokoyama, pp. 117–140, TERRA PUB, Tokyo.

Hutchison, I. (1985), The effects of sedimentation and compaction on oceanic heat flow, *Geophys. J. Int.*, *82*, 439–459, doi:10.1111/j.1365-246X.1985.tb05145.x.

Hyndman, R. D., and K. Wang (1995), The rupture zone of Cascadia great earthquakes from current deformation and the thermal regime, *J. Geophys. Res.*, *100*, 22,133–22,154, doi:10.1029/95JB01970.

Hyndman, R. D., J. P. Foucher, M. Yamano, A. T. Fisher, and the ODP Leg 131 Scientific Party (1992), Deep sea bottom simulating reflectors: Calibration of the base of the hydrate stability field as used for heat flow estimates, *Earth Planet. Sci. Lett.*, *109*, 289–301.

Hyndman, R. D., K. Wang, and M. Yamano (1995), Thermal constraints on the seismogenic portion of the southwestern Japan subduction thrust, *J. Geophys. Res.*, *100*, 15,373–15,392, doi:10.1029/95JB00153.

Ike, T., G. F. Moore, S. Kuramoto, J.-O. Park, Y. Kaneda, and A. Taira (2008), Variations in sediment thickness and type along the northern Philippine Sea Plate at the Nankai Trough, *Isl. Arc*, *17*, 342–357, doi:10.1111/j.1440-1738.2008.00624.x.

Ishii, T., H. Sato, S. Machida, S. Haraguchi, A. Usui, O. Ishizuka, H. Taniguchi, and K. Yagi (2000), Geological and petrological studies

of the Kinan and Izu-Ogasawara-back arc-echelon Seamount Chains [in Japanese with English abstract], *Bull. Geol. Surv. Jpn.*, *51*, 615–630.

Ito, Y., K. Obara, K. Shiomi, S. Sekine, and H. Hirose (2007), Slow earthquakes coincident with episodic tremors and slow slip events, *Science*, *315*, 503–506.

Kagami, H., et al. (1986), *Initial Reports of the Deep Sea Drilling Project*, vol. 87, 985 pp., U.S. Gov. Print. Off., Washington, D. C., doi:10.2973/dsdp.proc.87.1986.

Kanamori, H. (1972), Tectonic implications of the 1944 Tonankai and 1946 Nankaido earthquakes, *Phys. Earth Planet. Inter.*, *5*, 129–139, doi:10.1016/0031-9201(72)90082-9.

Karig, D. E., et al. (1975), *Initial Reports of the Deep Sea Drilling Project*, vol. 31, 927 pp., U.S. Gov. Print. Off., Washington, D. C., doi:10.2973/dsdp.proc.31.1975.

Kimura, J.-I., R. J. Stern, and T. Yoshida (2005), Reinitiation of subduction and magmatic responses in SW Japan during Neogene time, *Geol. Soc. Am. Bull.*, *117*(7–8), 969–986, doi:10.1130/B25565.1.

Kinoshita, H., and M. Yamano (1986), The heat flow anomaly in the Nankai Trough area, *Initial Rep. Deep Sea Drill. Proj.*, *87*, 737–743.

Kinoshita, M., and M. Yamano (1995), Heat flow distribution in the Nankai Trough region, in *Geology and Geophysics of the Philippine Sea Floor*, edited by S. A. Shcheka et al., pp. 77–86, TERRA PUB, Tokyo.

Kinoshita, M., T. Kanamatsu, K. Kawamura, T. Sibata, H. Hamamoto, and K. Fujino (2008), Heat flow distribution on the floor of Nankai Trough off Kumano and implications for the geothermal regime of subducting sediments, *JAMSTEC Deep-Sea Res.*, *8*, 13–28.

Kinoshita, M., H. J. Tobin, J. Ashi, G. Kimura, S. Lallemant, E. J. Screaton, D. Curewitz, H. Masago, K. T. Moe, and the Expedition 314/315/316 Scientists (2011a), Proceedings of the Integrated Ocean Drilling Program, *314*/*315*/*316*.

Kinoshita, M., G. F. Moore, and Y. N. Kido (2011b), Heat flow estimated from BSR and IODP borehole data: Implication of recent uplift and erosion of the imbricate thrust zone in the Nankai Trough off Kumano, *Geochem. Geophys. Geosyst.*, *12*, Q0AD18, doi:10.1029/2011GC003609.

Kobayashi, K., S. Kasuga, and K. Okino (1995), Shikoku basin and its margins, in *Back-Arc Basins*, edited by B. Taylor, pp. 381–405, Plenum, New York.

Kodaira, S., N. Takahashi, J. A. Park, K. Mochizuki, M. Shinohara, and S. Kimura (2000), Western Nankai Trough seismogenic zone: Results from a wide-angle ocean bottom seismic survey, *J. Geophys. Res.*, *105*, 5887–5905.

Kodaira, S., E. Kurashimo, J. Park, N. Takahashi, A. Nakanishi, S. Miura, T. Iwasaki, N. Hirata, K. Ito, and Y. Kaneda (2002), Structural factors controlling the rupture process of a megathrust earthquake at the Nankai Trough seismogenic zone, *Geophys. J. Int.*, *149*, 815–835, doi:10.1046/j.1365-246X.2002.01691.x.

Kvenvolden, K. A. (1993), Gas hydrates—Geological perspective and global change, *Rev. Geophys.*, *31*, 173–187.

Lin, W., O. Tadai,T. Hirose, W. Tanikawa, M. Takahashi, H. Mukoyoshi, and M. Kinoshita (2011), Thermal conductivities under high pressure in core samples from IODP NanTroSEIZE drilling site C0001, *Geochem. Geophys. Geosyst. 12*, Q0AD14, doi:10.1029/2010gc003449.

Lister, C. R. B. (1972), On the thermal balance of a mid-ocean ridge, *Geophys. J. R. Astron. Soc.*, *26*, 515–535.

Liu, Z., S. Owen, D. Dong, P. Lungren, F. Webb, E. Hetland, and M. Simmons (2010), Estimation of interplate coupling in the Nankai Trough, Japan using GPS data from 1996 to 2006, *Geophys. J. Int.*, *181*, 1313–1328, doi:10.1111/j.1365-246X.2010.04600.x.

Manea, V., M. Manea, V. Kostoglodov, C. Currie, and G. Sewell (2004), Thermal structure, coupling and metamorphism in the Mexican subduction zone beneath Guerrero, *Geophys. J. Int.*, *158*(2), 775–784.

Marcaillou, B. et al. (2012), Seismogenic zone temperatures and heat-flow anomalies in the Tonankai margin segment based on temperature data from IODP expedition 333 and thermal model, *Earth Planet. Sci. Lett.*, *349–350*, 171–185, doi:10.1016/j.epsl.2012.06.048.

Martin, V., P. Henry, H. Nouze, M. Noble, J. Ashi, and G. Pascal (2004), Erosion and sedimentation as processes controlling the BSR-derived heat flow on the Eastern Nankai margin, *Earth Planet. Sci. Lett.*, *222*, 131–144, doi:10.1016/j.epsl.2004.02.020.

McCaffrey, R. (1993), On the role of the upper plate in great subduction zone earthquakes, *J. Geophys. Res.*, *98*, 11,953–11,966, doi:10.1029/93JB00445.

McCaffrey, R. (1997), Influences of recurrence times and fault zone temperatures on the age-rate dependence of subduction zone seismicity, *J. Geophys. Res.*, *102*, 22,839–22,854, doi:10.1029/97JB01827.

Mikada, H., et al. (2002), *Proceedings of the Ocean Drilling Program, Initial Reports*, vol. 196, Ocean Drill. Program, College Station, Tex., doi:10.2973/odp.proc.ir.196.2002.

Miyake, Y., Y. Sugimura, and Y. Hirao (1975), Uranium, thorium, and potassium contents in granitic and basaltic rocks in Japan, in *The Natural Radiation Environment II*, pp. 535–558, Rice University, Houston, Tex.

Miyazaki, S., and K. Heki (2001), Crustal velocity field of southwest Japan: Subduction and arc-arc collision, *J. Geophys. Res.*, *106*, 4305–4326, doi:10.1029/2000JB900312.

Molnar, P., and P. England (1995), Temperatures in zones of steady-state underthrusting of young oceanic lithosphere, *Earth Planet. Sci. Lett.*, *131*, 57–70.

Moore, J. C., and D. Saffer (2001), Updip limit of the seismogenic zone beneath the accretionary prism of southwest Japan: An effect of diagenetic to low-grade metamorphic processes and increasing effective stress, *Geology*, *29*, 183–186, doi:10.1130/0091-7613(2001)029<0183:ULOTSZ>2.0.CO;2.

Moore, G. F., A. Taira, A. Klaus, and S. S. Party (2001), *Proceedings of the Ocean Drilling Program, Initial Reports*, vol. 190, Ocean Drill. Program, College Station, Tex., doi:10.2973/odp.proc.ir.190.2001.

Moore, G. F., at al. (2009), Structural and seismic stratigraphic framework of the NanTroSEIZE Stage 1 transect, *Proc. Integr. Ocean Drill. Program*, *314*/*315*/*316*, 1–46, doi:10.2204/iodp.proc.314315316.102.2009.

Müller, R. D., M. Sdrolias, C. Gaina, and W. R. Roest (2008), Age, spreading rates, and spreading asymmetry of the world's ocean crust, *Geochem. Geophys. Geosyst.*, *9*, Q04006, doi:10.1029/2007GC001743.

Nagihara, S., H. Kinoshita, and M. Yamano (1989), On the high heat flow in the Nankai Trough area—A simulation study on a heat rebound process, *Tectonophysics*, *161*, 33–41, doi:10.1016/0040-1951(89)90299-0.

Nakagawa, K., and K. Komatsu (1979), Thermal structure under the ground in Osaka Plain, southwest Japan, *J. Geosci.*, *22*, 151–166.

Nakajima, J., and A. Hasegawa (2007), Subduction of the Philippine Sea plate beneath southwestern Japan: Slab geometry and its relationship to arc magmatism, *J. Geophys. Res.*, *112*, B08306, doi:10.1029/2006JB004770.

Nakanishi, A., N. Takahashi, J. O. Park, S. Miura, S. Kodaira, Y. Kaneda, N. Hirata, T. Iwasaki, and M. Nakamura (2002), Crustal structure across the coseismic rupture zone of the 1944 Tonankai earthquake, the central Nankai Trough seismogenic zone, *J. Geophys. Res.*, *107*(B1), 2007, doi:10.1029/2001JB000424.

Obara, K. (2002), Nonvolcanic deep tremor associated with subduction in southwest Japan, *Science*, *296*, 1679–1681.

Obara, K., H. Hirose, F. Yamamizu, and K. Kasahara (2004), Episodic slow slip events accompanied by non-volcanic tremors in southwest Japan subduction zone, *Geophys. Res. Lett.*, *31*, L23602, doi:10.1029/2004GL020848.

Okino, K., Y. Shimakawa, and S. Nagaoka (1994), Evolution of the Shikoku Basin, *J. Geomagn. Geoelec.*, *46*, 463–479.

Okino, K., Y. Ohara, S. Kasuga, and Y. Kato (1999), The Philippine Sea: new survey results reveal the structure and the history of the marginal basins, *Geophys. Res. Lett.*, *26*, 2287–2290.

Oleskevich, D., R. Hyndman, and K. Wang (1999), The updip and downdip limits to great subduction earthquakes: Thermal and structural models of Cascadia, south Alaska, SW Japan, and Chile, *J. Geophys. Res.*, *104*(B7), 14,965–14,991.

Park, C.-H., K. Tamaki, and K. Kobayashi (1990), Age-depth correlation of the Philippine Sea back arc basins and other marginal basins in the world, *Tectonophysics*, *181*, 351–371.

Park, J.-O., T. Tsuru, S. Kodaira, P. R. Cummins, and Y. Kaneda (2002), Splay fault branching along the Nankai subduction zone, *Science*, *297*, 1157–1160.

Parsons, B., and J. G. Sclater (1977), An analysis of the variation of ocean floor bathymetry and heat flow with age, *J. Geophys. Res.*, *82*, 803–827.

Peacock, S. M., and K. Wang (1999), Seismic consequences of warm versus cool subduction metamorphism: Examples from southwest and northeast Japan, *Science*, *286*(5441), 937–939.

Pribnow, D., M. Kinoshita, and C. Stein (2000), Thermal data collection and heat flow recalculations for Ocean Drilling Program Legs 101–180, Inst. for Jt. Geosci. Res., Hannover, Germany. [Available at http://www-odp.tamu.edu/publications/heatflow/ODPReprt.pdf].

Sagiya, T., and W. Thatcher (1999), Coseismic slip resolution along a plate boundary megathrust: The Nankai Trough, southwest Japan, *J. Geophys. Res.*, *104*(B1), 1111–1129.

Saito, S., M. B. Underwood, Y. Kubo, and the Expedition 322 Scientists (2010), Leg 322 expedition reports, in *NanTroSEIZE Stage 2: Subduction Input, Proc. Integr. Ocean Drill. Program*, *322*.

Sass, J. H., A. H. Lachenbruch, and R. J. Munroe (1971), Thermal conductivity of rocks from measurements on fragments and its application to heat flow determinations, *J. Geophys. Res.*, *76*, 3391–3401, doi:10.1029/JB076i014p03391.

Sass, J. H., C. Stone, and R. J. Munroe (1984), Thermal-conductivity determinations on solid rock—A comparison between a steady-state divided-bar apparatus and a commercial transient line-source device, *J. Volcanol. Geotherm. Res.*, *20*, 145–153, doi:10.1016/0377-0273(84)90071-4.

Sato, H., S. Machida, S. Kanayama, H. Taniguchi, and T. Ishii (2002), Geochemical and isotopic characteristics of the Kinan Seamount Chain in the Shikoku Basin, *Geochem. J.*, *36*(5), 519–526.

Sdrolias, M., W. R. Roest, and R. D. Müller (2004), An expression of Philippine Sea plate rotation: The Parece Vela and Shikoku Basins, *Tectonophysics*, *394*, 69–86, doi:10.1016/j.tecto.2004.07.061.

Sella, G. F., T. H. Dixon, and A. Mao (2002), REVEL: A model for recent plate velocities from space geodesy, *J. Geophys. Res.*, *107*(B4), 2081, doi:10.1029/2000JB000033.

Seno, T., S. Stein, and A. E. Gripp (1993), A model for the motion of the Philippine Sea plate consistent with NUVEL-1 and geological data, *J. Geophys. Res.*, *98*, 17,941–17,948, doi:10.1029/93JB00782.

Shiomi, K., H. Sato, K. Obara, and M. Ohtake (2004), Configuration of subducting Philippine Sea plate beneath southwest Japan revealed from receiver function analysis based on the multivariate autoregressive model, *J. Geophys. Res.*, *109*, B04308, doi:10.1029/2003JB002774.

Shipboard Scientific Party (1975a), Site 297, *Initial Rep. Deep Sea Drill. Proj.*, *31*, 275–316, doi:10.2973/dsdp.proc.31.108.1975.

Shipboard Scientific Party (1975b), Site 298, *Initial Rep. Deep Sea Drill. Proj.*, *31*, 317–350, doi:10.2973/dsdp.proc.31.109.1975.

Shipboard Scientific Party (1986a), Site 582, *Initial Rep. Deep Sea Drill. Proj.*, *87*, 35–122, doi:10.2973/dsdp.proc.87.103.1986.

Shipboard Scientific Party (1986b), Site 583, *Initial Rep. Deep Sea Drill. Proj.*, *87*, 123–256, doi:10.2973/dsdp.proc.87.104.1986.

Shipley, T. H., M. H. Houston, R. T. Buffler, F. J. Shaub, K. J. McMillen, J. W. Ladd, and J. L. Worzel (1979), Seismic evidence for widespread possible gas hydrate horizons on continental slopes and rises, *Am. Assoc. Pet. Geol. Bull.*, *63*, 2204–2213.

Spinelli, G. A., and R. N. Harris (2011), Thermal effects of hydrothermal circulation and seamount subduction: Temperatures in the Nankai Trough Seismogenic Zone Experiment transect, Japan, *Geochem. Geophys. Geosyst.*, *12*, Q0AD21, doi:10.1029/2011GC003727.

Spinelli, G. A., and K. Wang (2008), Effects of fluid circulation in subducting crust on Nankai margin seismogenic zone temperatures, *Geology*, *36*(11), 887–890.

Spinelli, G. A., E. R. Giambalvo, and A. T. Fisher (2004), Sediment permeability, distribution, and influence on fluxes in oceanic basement, in *Hydrogeology of the Oceanic Lithosphere*, edited by E. E. Davis and H. Elderfield, pp. 151–188, Cambridge Univ. Press, New York.

Stein, C. A., and S. Stein (1992), A model for the global variation in oceanic depth and heat flow with lithospheric age, *Nature*, *359*, 123–129.

Stein, C. A., and S. Stein (1994), Constraints on hydrothermal heat flux through the oceanic lithosphere from global heat flow, *J. Geophys. Res.*, *99*, 3081–3095.

Taira, A., I. Hill, and J. Firth, (1991), *Proceedings of the Ocean Drilling Program Initial Results*, vol. 131, Ocean Drill. Program, College Station, Tex.

Takahashi, N., S. Kodaira, A. Nakanishi, J. Ä. Park, S. Miura, T. Tsuru, Y. Kaneda, K. Suyehiro, H. Kinoshita, and N. Hirata (2002), Seismic structure of western end of the Nankai trough seismogenic zone, *J. Geophys. Res.*, *107*(B10), 2212, doi:10.1029/2000JB000121.

Tanaka, A., M. Yamano, Y. Yano, and M. Sasada (2004), Geothermal gradient and heat flow data in and around Japan (I): Appraisal of heat flow geothermal gradient data, *Earth Planets Space*, *56*, 1191–1194.

Taylor, B. (1992), Rifting and the volcanic-tectonic evolution of the Izu-Bonin-Mariana arc, *Proc. Ocean Drill. Program Sci. Results*, *126*, 627–651.

Tobin, H., and M. Kinoshita (2006), NanTroSEIZE: The IODP Nankai Trough Seismogenic Zone Experiment, *Sci. Drill.*, *2*, 23–27, doi:10.2204/iodp.sd.2.06.2006.

Vacquier, V. (1985), The measurement of thermal conductivity of solids with a transient linear heat source on the plane surface of a poorly conducting body, *Earth Planet. Sci. Lett.*, *74*(2–3), 275–279, doi:10.1016/0012-821X(85)90027-5.

Van den Beukel, J., and R. Wortel (1988), Thermo-mechanical modelling of arc-trench regions, *Tectonophysics*, *154*, 177–193, doi:10.1016/0040-1951(88)90101-1.

Von Herzen, R. P., and A. E. Maxwell (1959), The measurement of thermal conductivity of deep-sea sediments by a needle-probe method, *J. Geophys. Res.*, *64*, 1557–1563, doi:10.1029/JZ064i010p01557.

Wada, I., and K. Wang (2009), Common depth of slab-mantle decoupling: Reconciling diversity and uniformity of subduction zones, *Geochem. Geophys. Geosyst.*, *10*, Q10009, doi:10.1029/2009GC002570.

Wang, K., R. D. Hyndman, and M. Yamano (1995), Thermal regime of the Southwest Japan subduction zone: Effects of age history of the subducting plate, *Tectonophysics*, *248*(1–2), 53–69.

Wang, K., I. Wada, and Y. Ishikawa (2004), Stresses in the subducting slab beneath southwest Japan and relation with plate geometry, tectonic forces, slab dehydration, and damaging earthquakes, *J. Geophys. Res.*, *109*, B08304, doi:10.1029/2003JB002888.

Wang, K., Y. Hu, and J. He (2012), Deformation cycles of subduction earthquakes in a viscoelastic Earth, *Nature*, *484*(7394), 327–332.

Watanabe, T., D. Epp, S. Uyeda, M. Langseth, and M. Yasui (1970), Heat flow in the Philippine Sea, *Tectonophysics*, *10*, 10,205–10,224, doi:10.1016/0040-1951(70)90107-1.

Watts, A. B., and J. K. Weissel (1975), Tectonic history of the Shikoku marginal basin, *Earth Planet. Sci. Lett.*, *25*, 239–250, doi:10.1016/0012-821X(75)90238-1.

Yamaguchi, T. I., M. Yamano, T. Nagao, and S. Goto (2001), Distribution of radioactive heat production around an active fault and in accretionary prisms of southwest Japan, *Phys. Earth Planet. Inter.*, *126*(3–4), 269–277, doi: 10.1016/s0031-9201(01)00260-6.

Yamano, M., and M. Kinoshita (1995), Heat flow in the Philippine Sea, in *Geology and Geophysics of the Philippine Sea Floor*, edited by S. A. Shcheka and H. Tokuyama, pp. 59–75, Terrapub, Tokyo.

Yamano, M., S. Uyeda, Y. Aoki, and T. H. Shipley (1982), Estimates of heat flow derived from gas hydrates, *Geology*, *10*, 339–343, doi:10.1130/0091-7613(1982)10<339:EOHFDF>2.0.CO;2.

Yamano, M., S. Honda, and S. Uyeda (1984), Nankai Trough: A hot trench?, *Mar. Geophys. Res.*, *6*, 187–203, doi:10.1007/BF00285959.

Yamano, M., J.-P. Foucher, M. Kinoshita, A. Fisher, R. D. Hyndman, O. D. P. Leg, and 131 Shipboard Scientific Party (1992), Heat flow and fluid flow regime in the western Nankai accretionary prism, *Earth Planet. Sci. Lett.*, *109*, 451–462.

Yamano, M., M. Kinoshita, S. Goto, and O. Matsubayashi (2003), Extremely high heat flow anomaly in the middle part of the Nankai Trough, *Phys. Chem. Earth, Parts A/B/C*, *28*(9–11), 487–497.

Yoshioka, S., and Y. Ito (2001), Lateral variations of effective elastic thickness of the subducting Philippine Sea plate along the Nankai Trough, *Earth Planets Space*, *53*, 261–273.

Yoshioka, S., and K. Murakami (2007), Temperature distribution of the upper surface of the subducted Philippine Sea plate along the Nankai Trough, southwest Japan, from a three dimensional subduction model: relation to large interplate and low-frequency earthquakes, *Geophys. J. Int.*, *171*, 302–315, doi:10.1111/j.1365-246X.2007.03510.x.

Zoth, G., and R. Haenel (1988), Appendix: 1, in *Handbook of Terrestrial Heat-Flow Density Determination: With Guidelines and Recommendations of the International Heat Flow Commission*, edited by R. Haenel, L. Rybach and L. Stegena, 449–466, Kluwer Acad., Dordrecht, Netherlands.